VISIBLE-NIR, ELECTRICAL IMPEDANCE, pH AND CIE L^*, a^* AND b^* COLOR SPACE VALUES TO PREDICT BEEF TENDERNESS

A Thesis

by

WILLIAM AL WIEDERHOLD

Submitted to the Office of Graduate Studies of
Texas A&M University
in partial fulfillment of the requirements for the degree of

MASTER OF SCIENCE

May 2011

Major Subject: Animal Science

Visible-NIR, Electrical Impedance, pH and CIE *L**, *a** and *b** Color Space Values to Predict Beef Tenderness

VISIBLE-NIR, ELECTRICAL IMPEDANCE, pH AND CIE *L**, *a** AND *b** COLOR SPACE VALUES TO PREDICT BEEF TENDERNESS

A Thesis

by

WILLIAM AL WIEDERHOLD

Submitted to the Office of Graduate Studies of
Texas A&M University
in partial fulfillment of the requirements for the degree of

MASTER OF SCIENCE

Approved by:

Co-Chairs of Committee,	Jeff Savell
	Rhonda Miller
Committee Members,	Dan Hale
	John Siebert
	Davey Griffin
Head of Department,	H. Russell Cross

May 2011

Major Subject: Animal Science

ABSTRACT

Visible-NIR, Electrical Impedance, pH and CIE *L**, *a** and *b** Color Space Values to Predict Beef Tenderness.

(May 2011)

William Al Wiederhold, B.S., Texas A&M University

Co-Chairs of Advisory Committee: Dr. Jeff Savell
Dr. Rhonda Miller

Predicting tenderness in today's beef supply could be advantageous to packers and consumers. In this study (n = 1,137 carcasses), visible-near-infrared, electrical impedance, pH and Minolta CIE *L**, *a**, and *b** color space values were examined as predictors of beef 1, 7, and 14 d Warner-Bratzler (N) or Slice Shear (N) force values as estimators of beef tenderness. Visible-NIR at 350 to 1830 nm, electrical impedance, and color space values were taken at the beef packing plant, along with carcass data. Strip loins were transported to Texas A&M University where pH was taken. Six steaks were taken from the anterior end of the strip loin and randomly assigned to either Warner-Bratzler shear force (WBSF) after 1, 7, or 14 days, or Slice shear force (SSF) after 1, 7, and 14 days of post-harvest aging at 2°C. Shears were taken on assigned days.

Shear force values were highly correlated with each other (r = 0.37 to 0.56 for WBSF and r = 0.75 to 0.78 for SSF) ($P < 0.05$). Within the independent variables, reflectance values for mid-range wavelengths (562nm-1193nm) were found to be most highly correlated with the dependent variables ($P < 0.05$). pH and color spaces values

were more highly correlated ($P < 0.05$) to slice shears values then to Warner-Bratzler shears force values. Electrical impedance was the least significant with r values of 0.00 to 0.14.

When Visble-NIR reflectance values were used in stepwise regression equations to predict 1, 7, or 14 d WBSF or 1, 7, or 14 d SSF, prediction equations for 14 d WBSF and SSF had the highest R^2 (0.14 and 0.36, respectively). Stepwise regression equations that included pH and color space values had the highest R^2 for 7 d WBSF and 1 d SSF (0.22 and 0.28, respectively). Electrical impedance alone in a stepwise regression equation had the highest R^2 for 1 and 14 d WBSF and 1 and 7 d SSF (0.02 and 0.03, respectively). Stepwise regression equations that included pH, color space values, and electrical impedance had the highest R^2 for 7 d WBSF and 14 d SSF (0.25 and 0.24, respectively). When pH, color space values, electrical impedance, and Visible-NIR were used, 7 d WBSF and 1 d SSF had the highest R^2 (0.38 and 0.34, respectively). Stepwise regression equations that included pH, color space values, and Visible-NIR had the highest R^2 for 7 d WBSF and 14 d SSF (0.30 and 0.44, respectively). For predicting 14 d Warner-Bratzler shear force, a R^2 of 0.20 was found using Visible-NIR, pH and color space values. When used, the partial least squares equation predicted tenderness with an 85 % success rate. For predicting 14 d Slice shear forces, a R^2 of 0.40 was found. When used, the partial least squares equation had a 100 % success rate of predicting those steaks found tender to be tender for Slice shear force. There was an 85 % success rate for predicting 14 d Warner-Bratzler shear forces. Both equations still had little to no success in predicting tough steaks. The Visible-NIR can successfully predict tenderness

and can be implemented in the plant. However, more research still needs to be conducted.

ACKNOWLEDGEMENTS

I would like to thank my committee co-chairs, Dr. Savell and Dr. Miller, and my committee members, Dr. Hale, Dr. Griffin, and Dr. Siebert, for their guidance and support throughout the course of this research.

Thanks also go to my friends and colleagues and the department faculty and staff for making my time at Texas A&M University a great experience. I also want to extend my gratitude to fellow graduate students, who provided countless hours of help at all times of days. If it were not for the help from fellow peers, the project would not have been completed.

Finally, thanks to my mother and father for their encouragement and to my wife for her patience and love.

TABLE OF CONTENTS

LIST OF FIGURES

Page

LIST OF TABLES

Page

CHAPTER I

INTRODUCTION

Beef is typically a high-priced protein source (Wulf, O'Connor, Tatum & Smith, 1997) and therefore, assurance of quality, specifically tenderness, is important in meeting consumer satisfaction (Boleman, Boleman, Miller, Taylor, Cross, Wheeler, Koohmaraie, Shackelford, Miller, West, Johnson & Savell, 1997; Shackelford, Wheeler, Meade, Reagan, Byrnes & Koohmaraie, 2001). Shackelford et al. (2001) found that consumers preferred the purchase of a branded program of guaranteed tender beef. They also reported that the consumers indicated that they would be willing to purchase all their meat at the same store if a beef source could be guaranteed tender. Additionally, Boleman et al. (1997) consumers were willing to pay a premium for guaranteed tender beef .

Wulf and Page (2000) proposed that changes should be made to the current USDA grading standards to incorporate automated grading technologies for tenderness assessment. Wulf and Page (2000) also stated that using the current USDA marbling standards to predict tenderness had a lower correlation than when using values from the colorimeter. In their study, they concluded that a color measurement could be used that could differentiate the tenderness of USDA Choice and USDA Select carcasses. The combined percentage of both the USDA Choice and USDA Select carcasses is 94.4% in the United States (Garcia, Nicholson, Hoffman, Lawrence, Hale, Griffin, Savell, VanOverbeke, Morgan, Belk, Field, Scanga, Tatum & Smith, 2008). With

---

This thesis follows the style of *Meat Science*.

the high percentage of carcasses falling into that range, being able to differentiate the more palatable carcasses within these grades would add value and give incentives to producers to look for ways to make beef more tender.

Guaranteed tender beef programs are emerging. Cargill Meat Solution (Wichita, KS) has Sterling Silver, and other premium Choice programs, and Nolan Ryan (Huntsville, TX) markets All Natural, Guaranteed Tender Beef. Since 1978, Certified Angus Beef, LLC has established its brand based on delivering a consistent, tender product since 1978. Multiple studies have been conducted examining Near-infrared spectroscopy (NIR) and Visible-Near-infrared spectroscopy (VIS-VISIBLE-NIR) technologies to predict beef tenderness (Park, Chen, Hruschka, Shackelford & Koohmaraie, 1998; Price, Hilton, VanOverbeke & Morgan, 2008; Rust, Price, Subbiah, Kranzler, Hilton, Vanoverbeke & Morgan, 2008; Shackelford, Wheeler & Koohmaraie, 2005; Wheeler, Vote, Leheska, Shackelford, Belk, Wulf, Gwartney & Koohmaraie, 2002). These studies focused on NIR and its ability to predict Warner-Bratzler and Slice shear force values.

The United States Department of Agriculture (USDA), Agricultural Marketing Service (AMS) has proposed labeling regulation for beef tenderness claims. Some companies including Nolan Ryan Tender Aged Beef already have begun marketing a guaranteed tender program with the help of the NIR technology. With the popularity of the new labeling regulations, the beef industry is aggressively seeking to implement the use of automated-grading technologies to accurately assess beef tenderness. It has also been a priority to make the NIR system more accurate, as well, as more convenient for

the industry to use. The current instruments and methods for determining palatability of meat has been destructive and/or time consuming (Liao, Fan & Cheng, 2010). Finding a non-invasive method or instrument that can be implemented at on-line speed is a key for the beef industry. This study focuses on predicting beef tenderness at 1, 7, and 14 d post-harvest. Using pH, color space values, electrical impedance, and Visible-NIR, collectively and separately, 1, 7, and 14 d tenderness can be predicted. The objectives in this study were to evaluate Visible-NIR, electrical impedance, pH and color space values singly or in combination to predict beef tenderness, and to determine correlations between Visible-NIR, electrical impedance, pH, color space values, and beef tenderness.

CHAPTER II

LITERATURE REVIEW

Many studies have been conducted using the instruments and technology in this current study. Researchers have used these technologies separately and in combination. Some work has shown to be useful in the industry where the instrument has become used. Reviewing this literature helped get an understanding of the technology being used and the success it had in studies.

BeefCam™ Technology

Since the 1970's, instrumental grading has been a topic in the beef industry (Cross & Whittaker, 1992). One of the earlier methods of instrumental prediction of tenderness was the BeefCam™ (Belk, 1999). Belk (1999) explained that the BeefCam™ works using measurements of lean and fat color reflectance, that are captured using Video Image Analysis images containing up to 250,000 data points per measurement. This technology was used with programs like Nolan Ryan Tender Aged Beef to predict tender carcasses from tough carcasses. L^*, a^* and b^* color space values were being used in the current study at focus. To explain what the color space values are, L^* measures the lightness axis, where 100 is white and 0 is black, a^* measures from green to red and b^* measures blue to yellow. Color measurements for tenderness have been studied. Wulf and Page (2000) found that both L^*, a^* and b^* color space values were correlated ($r = -0.42$, -0.39 and -0.41) with shear force values, and consumer palatability ($P < 0.05$). This study showed that color values had a high success rate for predicting tough steaks ($R^2 = 0.41$). In a different study, Wulf et al. (1997) concluded that color could be an

indicator of tenderness. Wulf et al. (1997) found that *b** and *L** color space values were the best indicators for beef tenderness. Wulf et al. (1997) presented R^2 values (R^2 = 0.18) for *L**, *b** and *a** color space values for predicting tenderness. In both studies, Wulf and Page (2000) Wulf et al. (1997) found that *b** color space values were a major indicator for predicting beef tenderness. Wyle, Vote, Roeber, Cannell, Belk, Scanga, Goldberg, Tatum, and Smith (2003) showed that the BeefCam™ could sort tender from tough carcasses. Wyle et al. (2003) showed that both models, one that is a regression equation that uses the BeefCam™ measurements as independent variables and the second model was used to add in the USDA quality grades, of the BeefCam™ predicted tender carcasses, but still predicted an average of 1.5% of actual tender carcasses as tough carcasses. The study also presented data that showed lean and fat color measurements were highly significant ($P < 0.05$) predictors in linear regression equation for beef tenderness prediction. Wyle et al. (2003) concluded that development and testing of a prototype instrument was warranted. Other studies have shown prediction to have as low as a 30.7% error in 100% certification for USDA Select carcasses using the BeefCam™ (Wheeler et al., 2002). Wheeler et al. (2002) concluded that indirect technologies, such as prototype BeefCam™ and colorimeter, had the most trouble in predicting tenderness in USDA Select carcasses.

Garcia et al. (2008) found that in 2005, 41.1% of all beef carcasses were graded USDA Select. With a high percentage of carcasses grading USDA Select, finding an instrument that is accurate in determining tenderness of USDA Select carcasses is important. Improvements have been made in the prototype BeefCam™, and studies

found this new version of the BeefCam™ separated carcasses into groups with a more uniform steak tenderness (Vote, Belk, Tatum, Scanga & Smith, 2003). This system used the visible light spectrum reflectance values and accurately decreased the chances of a consumer receiving a tough steak from a carcass that was guaranteed tender. Even with these findings, improvements are still needed in assessing tenderness with visible color spectrum instrument technology.

pH

Beef meat pH decreases during conversion of muscle to meat. Generally, pH and color can be linked. As pH decreases, meat color is lighter as stated by Wulf and Wise (1999). When meat pH is high, color is darker and in meat with excessively high pH, greater than 6.0, the meat is defined as dark cutting beef. Jones and Tatum (1994), Nath (2008), and Wulf and Page (2000) found that beef meat pH ranged from around 5.2 to 6.7 post harvest. As explained, pH varies and is generally correlated with color values (Wulf and Wise, 1999), studies have been done using pH and color space values to predict beef tenderness.

pH probes are intrusive and have to be inserted into the muscle of the carcass to measure meat pH. It is more desirable to develop automated grading systems that are not distructive or intrusive. Wulf and Page (2000) found that beef with pH values less than 5.45 were more tender and beef with pHs higher than 5.45 were tougher ($P < 0.05$). Shackelford, Koohmaraie, Whipple, Wheeler, Miller, Crouse, and Reagan (1991) found varied relationships with pH and tenderness. Their study concluded that a high pH at 9 h post-harvest resulted in beef with high Warner-Bratzler shear force values. When pH

was higher at 12 h post-harvest, lower 7 d Warner-Bratzler shear force values were found. Jeremiah et al. (1991) found relationships between pH and color. This study found that most tender carcasses ranged in pH from 5.8 to 6.19. These carcasses accounted for the majority of tender carcasses. Jeremiah et al. (1991) concluded that the removal of tough carcasses could be done by using this pH range ($P < 0.05$). pH has been shown to be a variable in regression equations to predict tenderness (Jones & Tatum, 1994). Jones and Tatum (1994) reported that the best equation to predict beef tenderness used pH and marbling and explained less variation in beef tenderness than marbling. pH had a partial R^2 value of 0.025 and a R^2 of 0.115. pH meters have been developed to use in the meat processing environment and are commonly used in the pork industry to assess pork carcass pH. However, insertion of a probe into meat results in destruction and could possibly introduce microorganisms and/or pathogens into the product. Development of non-destructive or nonintrusive instrument with as strong or stronger relationships to beef tenderness would provide a system that would reduce microbial cross-contamination.

Near-infrared

NIR instruments use the infrared region of the electromagnetic spectrum from about 800 to 2500 nm and is based on the principle that chemical bonds of organic molecules absorb or emit infrared light when their vibration state changes. The NIR system is a non-destructive system that collects the readings from the reflected light and transmits the information back to a computer rapidly. The Visible-NIR instrument being used in this study has a wider spectrum of light wavelengths allowing a broader range of

reflectance values available for use. The wavelengths are 350 nm to 1830 nm, therefore, including the visible light spectrum from 350 nm to 800 nm in combination with the VISIBLE-NIR spectrum. Since the VISIBLE-NIR instrument is measuring reflectance values from wavelengths 350 – 1830 nm, visible light will be included as it is from 350-800 nm on the spectrum. Using another instrument that measures in the same spectrum may aid in the predictability of the instrument. Our instrument was defined as Visible-NIR.

The VISIBLE-NIR instrument has been shown to accurately predict tenderness (Bowling, Vote, Belk, Scanga, Tatum & Smith, 2009; Geesink, Schreutelkamp, Frankhuizen, Vedder, Faber, Kranen & Gerritzen, 2003; Liao et al., 2010; Park et al., 1998; Price et al., 2008; Rødbotten, Nilsen & Hildrum, 2000; Rust et al., 2008; Shackelford, Wheeler & Koohmaraie, 2004; Shackelford et al., 2005; Vote et al., 2003). Shackelford, Wheeler, and Koohmaraie (2005) found NIR to be ideal for a processing company to predict a low slice-shear force. The NIR also had a high acceptance rating for predicting Warner-Bratzler shear force values (Bowling et al., 2009). Bowling et al. (2009) reported that, Warner-Bratzler shear force values were correlated with VISIBLE-NIR values ($r = -0.27$ and -0.34), and that both the visible and near infrared spectra reflectance values account for variation in beef tenderness prediction equations. They found R^2 values with infrared light at only 0.13-0.14. When the whole spectrum was combined, R^2 values ranged from 0.15-0.20. Park et al. (1998) found close to the same results for tenderness prediction. Park et al. (1998), however, had higher R^2 values from 0.63-0.67. Wavelengths from 1,100 to 2,498 nm were used by Park et al. (1998) The

authors also concluded that VISIBLE-NIR could predict Warner-Bratzler shear force values and be a non-destructive instrument in predicting beef tenderness. A similar machine was used in an Oklahoma State University study. Researchers found that VISIBLE-NIR scanning was a suitable option for in-plant sorting of carcasses into tenderness groups (Rust et al., 2008). Rust et al. (2008) found a 70 % success rate for sorting tough from tender carcasses. Another study conducted at Oklahoma State University looked at separating or sorting various beef cuts into tenderness categories. Price et al. (2008) found that carcasses could be separated into tenderness categories and could also be used in branded beef programs. Nath (2008) found similar finding in using an VISIBLE-NIR instrument and its ability to predict tenderness. Nath (2008) found that the VISIBLE-NIR instrument had the highest success rate in predicting tough carcasses. It was not successful in predicting the very tender carcasses ($R^2 = 0.26$). When matched or paired with electrical impedance, the VISIBLE-NIR's percentage for predicting more tender cattle increased along with the R^2 values ($R^2 = 0.47$).

The other type of VISIBLE-NIR, which has been used more often, involves inserting a probe into the muscle. This instrument was used by Shackelford et al. (2005) and by Rust et al. (2008). This VISIBLE-NIR instrument is manufactured by ASD (Analytical Spectral Devices) as is the instrument in our study. The instrument collects spectra from 350 to 2500 nm and has a probe that is inserted. This method has been proven to identify USDA Select carcasses as tender ($R^2 = 0.22$). Shackelford et al. (2005) also stated that this method might only be useful in a branded beef program for Select beef carcasses. This is said due to the discount of USDA Select carcasses are discounted and

there is a need to add value to that group. Shackelford et al (2005) stated that higher degrees of marbling could interfere with the accuracy of the VISIBLE-NIR instrument and recommended using the probe NIR instrument with USDA Choice or Select carcasses.

As stated earlier, for the last thirty years instrumental grading has been a priority and finding instruments that are less destructive instruments has been a priority. Liao et al. (2010) recently found a R^2 value higher than 0.757 for predicting pork quality using a probe based VISIBLE-NIR technology. There has been less research completed using a non-destructive VISIBLE-NIR technology at line speed in plants. When Liao et al. (2010) used a non-destructive VISIBLE-NIR technology they were unable to determine a high acceptability rating for predicting pork tenderness. This was due to the variation in the sub-sample measurements caused by noise. When de-noising was used, a higher R^2 value was found (0.97). The NIR measurements never have been taken at a standard time post-harvest in the previously cited studies. Most studies took the measurement at 24 to 48 h postmortem. The measurement times can range depending on the plant's chilling time prior to grading. Rødbotten et al. (2000) took the measurements at 2 to 30 h postharvest. They concluded that taking the measurements that early postharvest time would not produce an accurate predictor of final beef tenderness. These results indicated that color values are more consistent when carcasses are in full rigor (Rødbotten et al., 2000). It was concluded that oxidation can affect the accuracy and reading of the NIR. To insure the best readings, the carcass needs to be given time to fully bloom or for the myoglobin to oxygenate. Since the VISIBLE-NIR is using the

color spectrum, and is measuring reflectance from the surface of the meat, using a surface probe will get more accurate color readings as compared to inserting probes into meat that has not had time to oxygenate.

In our study, a wider spectrum of reflectance values are being used to understand reflectance value changes across a full range of the color spectrum. Trying to accurately predict tough carcasses is one of the goals of this study. Many studies have had little to no success in accurately predicting tough carcasses (Nath, 2008; Rust et al., 2008; Shackelford et al., 2005).

Electrical Impedance

Electrical impedance is currently used in the human medical field for body composition cell studies. Electrical impedance is a small handheld instrument that is low cost and fast, making it ideal for use in meat processing plant environments. Electrical impedance was used in an earlier study to predict beef palatability and tenderness (Wulf & Page, 2000). However, Wulf and Page (2000) found little to no relationship between electrical impedance and beef palatability. Electrical impedance has been shown to be influenced by post-rigor aging (Lepetit, Salé, Favier & Dalle, 2002). This is due to the decrease in the anisotropy which occurs during aging when the electrical properties are changing. After aging, meat will turn isotropic, and the chance to measure the muscle fiber mechanical resistance decreases. Four measurements are obtained from electrical impedance. They are: resistance, reactance, phase angle and partial capacitance. The resistance is the measurement or reading that impedance is transmitting from the steak. Lepetit et al. (2002) found low relationships between

muscle collagen content and tenderness, and also showed low relationships between electrical readings and tenderness. Lepetit et al. (2002) and Wulf and Page (2000) did mentioned that impedance was able to assist, along with other instruments, in predicting tenderness. Very little research has been done using this instrument in combination with other technologies or factors. The findings of Lepetit et al. (2002), however, was contradicted by a recent study performed by Nath (2008). Nath (2008) found that the readings for days 5 and 14 on individual steaks were more accurate for tenderness compared to readings at day 4 on the carcasses exposed lean surface. When paired with NIR and its high success rate for predicting tough carcasses, electrical impedance was additive in the higher success rates for predicting beef tenderness reported by Nath (2008). Nath (2008) concluded that the reason predictability was up was due to NIR's ability to predict tough carcasses, and electrical impedance's ability at identifying tender carcasses.

In our study multiple instruments will be used to predict tenderness. Studies have been conducted using the NIR to predict tenderness. However, combining this technology with electrical impedance, L^*, a^* and b^* color space values, and pH could provide a more accurate method in predicting beef tenderness.

This study focused on two instrumental systems for predicting tenderness, visible-near-infrared spectroscopy (Visible-NIR) and electrical impedance (EI). In addition, color and pH were evaluated, which has been shown to have a moderately high correlation for predicting tenderness (Wulf & Page, 2000). These instruments will be used singly or in combination to predict 7 and 14 d beef tenderness with beef tenderness defined as Warner-Bratzler and Slice shear force tenderness.

CHAPTER III

MATERIALS AND METHODS

Cattle Source and Carcass Grading

In a 2 year study, beef carcasses from approximately 1,008 steers and heifers from Deseret Ranches and Rex Ranch, and 125 Santa Gertrudis heifer carcasses from the King Ranch were utilized. The cattle were either full *Bos taurus* or a *Bos taurus* crossed with *Bos indicus*. The cattle were fed a high-energy corn-based diet at the Texas A&M Research Center in McGregor, TX to a 1.0 cm fat constant endpoint. The cattle were transported to Sam Kane Beef Processors, Inc., Corpus Christi, Texas for harvest. Fat thickness of was estimated using definite system ultrasound. At 48 h post-harvest, one carcass side was ribbed at the 12^{th} rib interface, and experienced graders obtained carcass data. Skeletal maturity was based on visual aspects vertebrae and ribs and lean maturity was accessed on color of the 12^{th} rib interface, 12^{th} rib Fat depth (mm) ribeye area (cm^2) estimated kidney, pelvic, and heart fat %, and USDA marbling score at the 12^{th} rib (100 = Practically Devoid^{00}; 200 = Traces^{00};300 = Slight^{00}; 400 = Small^{00}; 500 = Modest^{00}; 600 = Moderate^{00}; 700 = Slightly Abundant^{00}; 800 = Moderately Abundant^{00}) where determined and USDA Yield and Quality grades were calculated (USDA, 1997).

Instrument Assessment

Following carcass grading, the right carcass side was evaluated at the 12^{th} rib lean

surface using the VISIBLE-NIR, electrical impedance, and Minolta CIE *L**, *a**, and *b** color space values. The VISIBLE-NIR data was obtained using a QualitySpec® BT (Analytical Spectral Devices, Boulder, CO) and three readings were taken by placing the light source head on the lean surface and taking three consecutive readings. The three readings were individual reflectance values from 350 nm to 1830 nm wavelengths. The three readings per carcass were averaged within a wavelength. The instrument was calibrated each day by placing the head on a standard white plate. An electrical impedance e-Fresh instrument (RJL Systems, Clinton, MI) was used. The four probes were placed on the lean cut surface of the 12th rib lean surface. The single reading of resistance, reactance, phase angle, and partial capacitance was reported. A color reading was taken using a Minolta Colorimeter (Konica-Minolta Cr-400, Ramsey, NJ) that was calibrated using a standard white plate, every twenty carcasses. Duplicate CIE *L**, *a**, and *b** color space values was obtained on the lean cut surface of the 12th rib lean surface. The average values of the two readings within a carcass were used in analysis.

Product Selection

After evaluation, NAMP 180 strip loins (NAMP, 2010) were removed from the right side of each carcass. The strip loins then were transported to Texas A&M University's Rosenthal Meat Science and Technology Center (College Station, TX) and stored at 2°C. Upon arrival, pH was taken using an IQ 150 pH meter (IQ Scientific Instruments, Inc. Carlsbad, CA) in the posterior end of the *longissimus* muscle to avoid affecting the tenderness in the anterior end with the probes. The reading was taken in duplicate and

averaged to determine the final pH. The pH meter was calibrated every 25 samples using buffer solutions of 4.0 and 7.0. One 1.27-cm steak and six 2.54-cm steaks were obtained beginning at the 13th rib and moving posterior. The 1.27 cm steak was used for lipid and moisture analysis. From the remaining six steaks from each loin, two steaks were assigned randomly to aging at 1, 7, or 14 d. Within an aging time, one steak was randomly assigned to either Warner-Bratzler (WBSF) or Slice shear force analysis. Steaks were vacuum-packaged in Cryovac® bags with an oxygen transfer rate < 150 and stored at 2°C for the defined aging time prior to tenderness measurements.

Steak Cooking

At the beginning of each of the assigned days, the steaks were removed from the cooler and package, assigned numeric numbers (randomly), and weighed before cooking. Steaks had a copper-constantan type T thermocouple (Omega Engineering, Inc. Stamford, CT) inserted into the geometric center, and the temperature was monitored using an Omega HH501BT (Omega Engineering, Inc. Stamford, CT) handheld thermometer. The steaks then were cooked to an internal temperature of 70°C using a Hamilton Beach (Hamilton Beach/Proctor-Silex, Inc. Southern Pines, NC) open face grill set at 177°C. Steaks were turned once at 35°C during cooking. The Warner-Bratzler shear force assigned steaks were allowed to rest, covered with Saran™ and come to room temperature for 4 h. After the end of 4 h, six cores were taken from each steak parallel to the longitudinal orientation of the muscle fibers. The cores were sheared perpendicular to the longitudinal orientation of the muscle fibers with a Warner-Bratzler shear attachment on a United SSTM-500 (United Calibration Corporation,

Huntington Beach, CA) with a head speed of 200 mm per minute, and a 10.0 kg load cell. The maximum force to segment a core was recorded (kg). The average value of cores within a steak was used as the WBSF value. The slice shear steaks were cooked to an internal temperature of 70°C using a Hamilton Beach open face grill set at 177°C, and following the same process as the Warner-Bratzler shear force assigned steaks. Without any time to rest, two slice samples were taken from each steak, parallel to the longitudinal orientation of the muscle fibers using a box with parallel slots and a dual bladed knife. The slice samples were sheared using a flat blunt blade (Shackelford, Wheeler & Koohmaraie, 1999b) attached to a United SSTM-500 (United Calibration Corporation, Huntington Beach, CA), The samples were sheared at a rate of 500 mm per minute using a 226.80 kg load cell, perpendicular to the longitudinal orientation of the muscle fibers. These readings were recorded in kilograms. The average of the two readings were used as the SSF for each steak.

Statistical Analysis

The data set was divided into the prediction and calibration data sets by sorting the data by 14 d Warner-Bratzler shear force. The first and every other animal were assigned to the prediction data set. The remaining animals were assigned to the calibration data set. Descriptive statistics were reported for the prediction and calibration data sets. Dependent variables were defined as 1, 7, and 14 d Warner-Bratzler shear forces, and 1, 7, and 14 d Slice shear force. Independent variables were defined as pH, CIE L^*, a^*, and b^* color space values, resistance, reactance, phase angle, partial capacitance, and VISIBLE-NIR reflectance values from individual wavelengths

at 350nm to 1830 nm. Simple correlations were determined between, dependent and independent variables. The 14 d Warner-Bratzler shear force values were classified into tough (≥ 3.9 kg), intermediate (< 3.9 kg and > 2.7 kg), and tender categories (≤ 2.7 kg). Stepwise regression was used to determine linear regression using SAS (v9.2, SAS Institute, Inc, Cary, NC). Final stepwise linear regression equation was inserted into Microsoft Excel (Microsoft Excel 2010) to determine the predicted Warner-Bratzler and Slice shear force values using the Calibration data set. The percent accuracy was calculated using the number of actually classified compared to the correctly predicted. The inflection points along the spectrum of the reflectance values were used to determine the differences. This was the method to try and condense the data to understand what segments of the spectrum had predictive values. Figure 1 shows the graph taken from those particular values described and plotted. A similar graph was developed by Bowling et al. (2009) and showed a similar output. The lines represent the tough, tender and mean of most all steaks. The highest and lowest points on the spectrum were to give the differences for all inflection points. A total of 14 differences were found from 15 inflection points. The differences were defined as Difference1 = 350nm reflectance - 404nm reflectance; Difference2 = 404nm reflectance - 512nm reflectance; Difference3 = 512nm reflectance - 542nm reflectance; Difference4 = 542nm reflectance -562nm reflectance; Difference5 = 562nm reflectance - 577nm reflectance; Difference6 = 577nm reflectance - 704nm reflectance; Difference7 = 704nm reflectance - 766nm reflectance; Difference8 = 766nm reflectance - 792nm reflectance; Difference9 = 792nm reflectance - 983nm reflectance; Difference10 = 983nm reflectance -1079nm

reflectance; Difference11 = 1079nm reflectance - 1193nm reflectance; Difference12 = 1193nm reflectance - 1265nm reflectance; Difference13 = 1265nm reflectance - 1458nm reflectance; Difference14 = 1458nm reflectance - 1830nm reflectance. These Differences and inflection points were used to help predict Warner-Bratzler and Slice shear forces. Partial least square regression was calculated using Unscrambler v 10.0 (CAMO, Inc. Woodbridge, NJ).

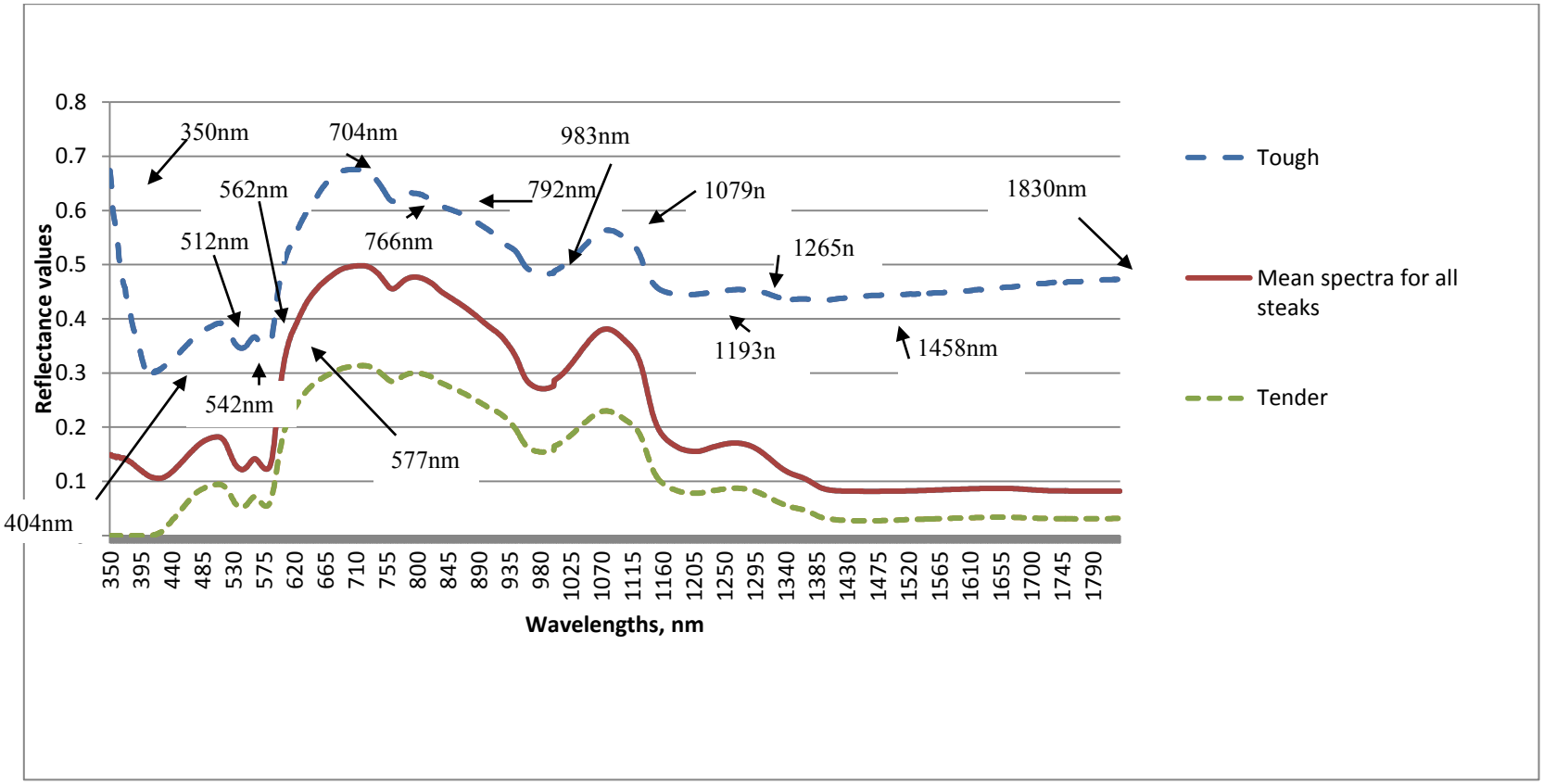

Figure 1.
Reflectance values taken by the ASD Quality Spec® BT showing the spectrum for the toughest, and most tender steaks and the mean spectra for the steaks in the study.

CHAPTER IV

CONCLUSION, RESULTS AND DISCUSSION

The n, means, standard deviations, minimum and maximum values for carcass data from the prediction and calibration data sets are reported in Table 1. Compared to the 2005 National Beef Quality Audit (Garcia et al., 2008; Rust et al., 2008), our data are similar in adjusted fat thickness, KPH, marbling score, USDA yield grade, and USDA quality grade. However, carcasses in our study were lighter with smaller ribeye areas than those reported by Garcia et al. (2008). Wulf and Page (2000) and Shackelford et al. (2004) used carcasses with similar carcass characteristics as our study to predict beef tenderness using pH, color, and electrical impedance. While our study had slightly lighter carcasses with smaller ribeye areas, these data are representative of carcasses within the beef industry and are an acceptable population to evaluate beef tenderness technologies.

Table 1
Descriptive statistics for prediction and calibration data sets for carcass characteristics.

Variables	*n*	Mean	SD	Minimum	Maximum
Prediction data set					
Carcass weight (kg)	567	301.6	29.58	205.7	382.1
Adjusted fat thickness (cm)	567	13.3	4.38	3.0	28.5
Ribeye Area (cm^2)	567	77.1	9.02	52,3	113.6
KPH (%)[a]	567	2.2	0.59	0.50	4.0
Marbling score[b]	567	423.51	89.72	270.0	880.0
USDA quality qrade	567	402.8	36.92	285.0	560.0
USDA yield grade[c]	567	2.92	0.70	-0.47	5.06
Calibration data set					
Carcass weight (kg)	566	304.7	27.72	176.1	376.6
Adjusted fat thickness (cm)	563	13.1	4.49	2.0	28.4
Ribeye Area (cm^2)	563	78.0	9.06	39.4	118.7
KPH (%)[a]	563	2.1	0.56	0.00	5.0
Marbling score[b]	563	426.0	83.27	180.0	780.0
USDA quality grade	563	403.7	35.66	267.0	526.7
USDA yield grade[c]	563	2.89	0.56	0.00	5.04

[a] Percent kidney, pelvic and heart fat.
[b] Marbling Score: 100=Practically Devoid[00]; 200=Traces[00];300=Slight[00]; 400=Small[00]; 500=Modest[00]; 600=Moderate[00]; 700=Slightly Abundant[00]; 800=Moderately Abundant[00].
[c] USDA (1997) yield grades based on five-point scale with yield grade 1 being the highest cutability and yield grade 5 being the lowest.

Simple statistics for the calibration and prediction data sets are reported in Tables 2 and 3. Brooks et al. (2000) showed similar Warner-Bratzler shear force values (28.64 N) in the National Beef Tenderness Survey when compared to Tables 2 and 3. Wulf et al. (1997) reported a mean of 26.2 N for Warner-Bratzler shear force values. However, Shackelford et al. (2005) reported a higher Slice shear force value of 186.4 N for 14 d aged steaks then reported for our study. pH values are similar to those reported by Wulf et al. (1997; 2000). However, the color space values are different than those reported in the studies by Wulf (1997; 2000). Wheeler et al. (2002) showed similar *L** values to

Wulf (2000). Additionally Wheeler et at. (2002) reported different a^* and b^* values than our study. These differences may be attributed to plant cooling and harvesting differences between the studies. While slight differences in mean and standard deviation may have been reported between our study and those for other studies used to predict beef tenderness, the range, variation, and mean for color and tenderness measurements indicate that prediction models developed using these data should be applicable to beef carcasses in the US. Values from our study are over multiple processing days and over two years and are most likely representative of values obtained from Same Kanes Beef Processors. Our values were within range and are still applicable to industry product and tenderness studies.

Table 2
Descriptive statistics for the prediction data set.

Variable	*n*	Mean	SD	Minimum	Maximum
Dependent variables					
Warner-Bratzler shear force, 1 d, N	566	30.90	10.17	13.70	73.43
Warner-Bratzler shear force, 7 d, N	564	24.58	7.38	12.76	65.33
Warner-Bratzler shear force, 14 d, N	563	22.76	6.00	11.55	66.85
Slice shear force, 1 d, N	562	158.85	72.32	50.36	429.77
Slice shear force, 7 d, N	559	118.28	52.17	32.70	368.70
Slice shear force, 14 d, N	564	106.05	41.64	38.96	385.07
Independent Variables					
pH	474	5.50	0.07	5.29	5.79
*L**	351	45.85	2.73	35.98	54.05
*a**	351	17.31	2.97	10.03	27.36
*b**	351	8.52	2.91	2.20	13.74
Resistance	361	75.45	8.71	54.60	106.90
Reactance	361	45.10	6.11	24.80	71.50
Phase angle	361	31.07	3.73	21.10	72.60
Partial capacitance	361	19397.24	9937.49	12169.70	200493.00
350 nm reflectance	567	0.15	0.09	0.00	0.67
404 nm reflectance	567	0.11	0.04	0.00	0.30
512 nm reflectance	567	0.18	0.03	0.09	0.37
542 nm reflectance	567	0.12	0.03	0.06	0.35
562 nm reflectance	567	0.14	0.03	0.07	0.36
577 nm reflectance	567	0.12	0.03	0.06	0.35
704 nm reflectance	567	0.49	0.06	0.31	0.67
766 nm reflectance	567	0.45	0.05	0.28	0.61
792 nm reflectance	567	0.47	0.05	0.30	0.63
983 nm reflectance	567	0.27	0.03	0.15	0.45
1079 nm reflectance	567	0.38	0.04	0.23	0.54
1193 nm reflectance	567	0.16	0.03	0.08	0.44
1265 nm reflectance	567	0.17	0.03	0.09	0.45
1458 nm reflectance	567	0.08	0.03	0.03	0.44
1830 nm reflectance	567	0.08	0.03	0.03	0.47
Difference1 [a]	567	0.04	0.06	-0.10	0.41
Difference2 [a]	567	-0.07	0.03	-0.23	0.05
Difference3 [a]	567	0.06	0.01	0.03	0.10
Difference4 [a]	567	-0.02	0.00	-0.04	-0.01
Difference5 [a]	567	0.02	0.00	0.01	0.04
Difference6 [a]	567	-0.37	0.04	-0.49	-0.20
Difference7 [a]	567	0.04	0.01	0.02	0.06
Difference8 [a]	567	-0.02	0.01	-0.04	-0.00
Difference9 [a]	567	0.21	0.02	0.09	0.28
Difference10 [a]	567	-0.11	0.01	-0.15	-0.07
Difference11 [a]	567	0.22	0.02	0.09	0.29
Difference12 [a]	567	-0.01	0.01	-0.06	-0.01
Difference13 [a]	567	0.09	0.02	0.01	0.15
Difference14 [a]	567	-0.00	0.00	-0.03	0.01

[a] These represent slope calculations of reflectance values between two wavelength measurements. Difference1 = 350nm reflectance -404nm reflectance; Difference2 = 404nm reflectance -512nm reflectance; Difference3 = 512nm reflectance -542nm reflectance; Difference4 = 542nm reflectance -562nm reflectance; Difference5 = 562nm reflectance -577nm reflectance; Difference6 = 577nm reflectance -704nm reflectance; Difference7 = 704nm reflectance -766nm reflectance; Difference8 = 766nm reflectance -792nm reflectance; Difference9 = 792nm reflectance -983nm reflectance; Difference10 = 983nm reflectance -1079nm reflectance; Difference11 = 1079nm reflectance -1193nm reflectance; Difference12 = 1193nm reflectance -1265nm reflectance; Difference13 = 1265nm reflectance -1458nm reflectance; Difference14 = 1458nm reflectance -1830nm reflectance.

Table 3
Descriptive statistics for calibration data sets.

Variable	*n*	Mean	SD	Minimum	Maximum
Dependent variables					
Warner-Bratzler shear force, 1 d, N	565	30.89	10.46	14.15	73.02
Warner-Bratzler shear foce, 7 d, N	562	24.43	7.69	12.95	65.33
Warner-Bratzler shear force, 14 d, N	562	22.74	5.85	12.31	58.94
Slice shear force, 1 d, N	562	158.07	65.76	50.53	525.97
Slice shear force, 7 d, N	561	121.68	52.20	35.40	432.14
Slice shear force, 14 d, N	561	110.72	45.58	36.66	290.56
Independent Variables					
pH	488	5.50	0.09	5.33	5.99
*L**	366	45.75	2.87	30.23	53.85
*a**	366	17.07	2.92	10.65	36.68
*b**	366	8.41	2.25	2.09	14.19
Resistance	370	74.39	8.52	54.20	117.60
Reactance	370	44.22	5.72	27.30	73.40
Phase angle	370	30.87	2.92	22.40	49.90
Partial capacitance	370	19091.88	2569.60	12214.10	27199.70
350 nm reflectance	566	0.15	0.08	0.00	0.48
404 nm reflectance	566	0.11	0.04	0.00	0.29
512 nm reflectance	566	0.18	0.04	0.10	0.39
542 nm reflectance	566	0.12	0.03	0.05	0.35
562 nm reflectance	566	0.14	0.03	0.07	0.37
577 nm reflectance	566	0.12	0.03	0.05	0.35
704 nm reflectance	566	0.50	0.06	0.34	0.68
766 nm reflectance	566	0.46	0.05	0.32	0.62
792 nm reflectance	566	0.48	0.05	0.34	0.63
983 nm reflectance	566	0.27	0.04	0.19	0.48
1079 nm reflectance	566	0.38	0.04	0.27	0.56
1193 nm reflectance	566	0.16	0.03	0.09	0.37
1265 nm reflectance	566	0.17	0.03	0.11	0.40
1458 nm reflectance	566	0.08	0.03	0.03	0.36
1830 nm reflectance	566	0.08	0.03	0.03	0.38
Difference1[a]	566	0.04	0.05	-0.11	0.27
Difference2[a]	566	-0.07	0.03	-0.20	0.03
Difference3[a]	566	0.06	0.01	0.02	0.10
Difference4[a]	566	-0.02	0.00	-0.03	-0.01
Difference5[a]	566	0.02	0.00	0.01	0.03
Difference6[a]	566	-0.37	0.04	-0.50	-0.19
Difference7[a]	566	0.04	0.01	0.02	0.06
Difference8[a]	566	-0.02	0.01	-0.04	-0.01
Difference9[a]	566	0.21	0.02	0.09	0.28
Difference10[a]	566	-0.11	0.01	-0.14	-0.07
Difference11[a]	566	0.22	0.02	0.11	0.29
Difference12[a]	566	-0.01	0.01	-0.06	-0.00
Difference13[a]	566	0.09	0.02	0.03	0.15
Difference14[a]	566	-0.00	0.00	-0.02	0.01

[a] These represent slope calculations of reflectance values between two wavelength measurements. Difference1 = 350nm reflectance -404nm reflectance; Difference2 = 404nm reflectance -512nm reflectance; Difference3 = 512nm reflectance -542nm reflectance; Difference4 = 542nm reflectance -562nm reflectance; Difference5 = 562nm reflectance -577nm reflectance; Difference6 = 577nm reflectance -704nm reflectance; Difference7 = 704nm reflectance -766nm reflectance; Difference8 = 766nm reflectance -792nm reflectance; Difference9 = 792nm reflectance -983nm reflectance; Difference10 = 983nm reflectance -1079nm reflectance; Difference11 = 1079nm reflectance -1193nm reflectance; Difference12 = 1193nm reflectance -1265nm reflectance; Difference13 = 1265nm reflectance -1458nm reflectance; Difference14 = 1458nm reflectance -1830nm reflectance.

Simple correlation coefficients for the prediction data set between dependent variables are found in Table 4. Aging time affected correlations between Warner-Bratzler and Slice shear force. As aging time increased, correlation coefficients values between Warner-Bratzler and Slice shear forces decreased. This may be due to the variability in steak's muscle degradation while aging occurred. For 1 d aged steaks, Warner-Bratzler and Slice shear force values were highly correlated. As aging took place and muscle fiber degradation occurred, steaks improved in tenderness and decreased in tenderness variation. Differences in aging rates with time most likely contributed to lower simple correlation coefficients between Warner-Bratzler and Slice shear force values. For both prediction and calibration data sets, there was a high correlation (0.59 and 0.63, respectively) between Slice shear force values and Warner-Bratzler shear force values for 1 d age. This correlation decreased for 14 d Warner-Bratzler and Slice shear force values (0.33 and 0.34 respectively). Similar relationships were found in the calibration data set in Table 5.

Table 4
Simple correlation coefficients for dependent variables from the prediction data set.[a]

Variable	Warner-Bratzler shear force 1d, N	Warner-Bratzler shear force 7d, N	Warner-Bratzler shear force 14d, N	Slice shear force 1d, N	Slice shear force 7d, N
Warner-Bratzler shear force, 7 d, N	0.59				
Warner-Bratzler shear force, 14 d, N	0.37	0.56			
Slice shear force, 1 d, N	0.59	0.60	0.38		
Slice shear force, 7 d, N	0.48	0.61	0.36	0.78	
Slice shear force, 14 d, N	0.44	0.49	0.33	0.75	0.76

[a] All *P*-values are significant ($P < 0.05$).

Simple correlation coefficients between independent variables for the prediction data set are found in table on page 29. Wulf et al. (1997) found high correlations between pH and color (-0.48, -0.52, and -0.60 for *L**, *a** and *b** color space values, respectively). In

our study, pH was not strongly correlated ($P < 0.05$) with the L^*, a^* and b^* color space values. pH and color can generally be linked (Wulf and Wise, 1999). Wulf and Wise (1999) reported correlations of -.57, -.79, and -.78, respectively for L^*, a^* and b^* color values with pH. It is generally known that when pH decreases muscle color gets lighter, and when pH increases, muscle color gets darker. Jeremiah et al. (1991) found that L^*, a^* and b^* color measurements accounted for up to 75 % of the variation in pH. Abril et al. (2001) showed that pH had the highest correlation with L^* and b^* color space values. When compared with electrical impedance, pH had the lowest simple correlation coefficients (0.02 to 0.10, respectively). Nearly all the VISIBLE-NIR reflectance values along with the difference variables were found to be correlated with pH ($P < 0.05$).

Table 5
Simple correlation coefficients for dependent variables from the calibration data set.[a]

Variable	Warner-Bratzler shear force 1d, N	Warner-Bratzler shear force 7d, N	Warner-Bratzler shear force 14d, N	Slice shear force 1d, N	Slice shear force 7d, N
Warner-Bratzler shear force, 7 d, N	0.66				
Warner-Bratzler shear force, 14 d, N	0.48	0.60			
Slice shear force, 1 d, N	0.63	0.57	0.33		
Slice shear force, 7 d, N	0.52	0.58	0.34	0.71	
Slice shear force, 14 d, N	0.42	0.46	0.34	0.70	0.72

[a] All *P*-values are significant ($P < 0.05$).

In Table 6, simple correlation coefficients for L^*, a^* and b^* color space values are reported. L^* color space values were the only color space value to have a high correlation with electrical impedance values (resistance, phase angle and partial capacitance). L^*, a^* and b^* color space values were not highly correlated with VISIBLE-NIR reflectance values at lower and higher wavelengths. L^* color space values were correlated with the reflectance values from the mid-range wavelengths of 704 - 1079 nm reflectance. L^*, a^* and b^* color space values had higher correlations with the Difference values 4, 5, 6, 7, and 8. L^* color space values were more highly

correlated with difference values. In our study, higher correlations of color space values with the midrange VISIBLE-NIR reflectance values is most likely due to *L*, a** and *b** color space values being measurements of the visible spectrum. *L** measures dark to light, *a** measures green to red, and b* measures blue to yellow (AMSA). Since visible light includes 350 – 800 nm wavelengths, higher correlation with VISIBLE-NIR reflectance values at the mid to lower wavelengths with color space values would be expected. Fewer correlations have been reported between pH and color space values, Wulf et al. (1997) did report higher correlations between color and pH. Similar values are found in the table for the calibration data on page 31. Based on the correlations, pH and *L*, a** and *b** color space values can be expected to contribute in predicting tenderness when used with VISIBLE-NIR reflectance values.

Table 6
Simple correlations coefficients between independent variables for the prediction data.

Variables	pH[a]	L^*[b]	a^*[b]	b^*[b]	Resistance[c]	Reactance[c]	Phase angle[c]	Partial capacitance[c]
L^*	0.10							
a^*	0.07	-0.05						
b^*	-0.09	-0.15	0.81					
Resistance	-0.02	0.16	-0.03	-0.01				
Reactance	0.02	0.03	-0.15	-0.03	0.58			
Phase angle	0.10	-0.13	-0.12	-0.01	-0.15	0.50		
Partial capacitance	0.05	-0.18	-0.03	0.00	-0.26	-0.04	0.15	
350 nm reflectance	0.04	-0.12	0.02	-0.02	-0.19	-0.00	0.17	0.05
404 nm reflectance	-0.01	-0.13	-0.07	-0.09	-0.19	-0.02	0.12	0.03
512 nm reflectance	-0.12	0.15	-0.05	-0.04	0.07	0.01	-0.06	-0.08
542 nm reflectance	-0.10	0.01	-0.11	-0.07	-0.00	-0.01	-0.03	-0.06
562 nm reflectance	-0.12	-0.08	-0.08	-0.05	0.04	-0.01	-0.05	-0.07
577 nm reflectance	-0.11	0.02	-0.10	-0.07	0.00	-0.02	-0.04	-0.06
704 nm reflectance	-0.09	0.33	0.11	0.03	0.13	-0.05	-0.16	-0.09
766 nm reflectance	-0.10	0.31	0.10	0.03	0.14	-0.04	-0.15	-0.09
792 nm reflectance	-0.11	0.28	0.04	-0.01	0.14	-0.03	-0.15	-0.10
983 nm reflectance	-0.12	0.13	-0.01	-0.02	0.08	-0.03	-0.08	-0.09
1079 nm reflectance	-0.11	0.14	-0.03	-0.05	0.08	-0.06	-0.11	-0.10
1193 nm reflectance	-0.08	0.01	-0.04	-0.05	-0.05	-0.11	-0.06	-0.06
1265 nm reflectance	-0.09	0.04	-0.03	-0.04	-0.01	-0.08	-0.05	-0.07
1458 nm reflectance	-0.04	-0.12	-0.11	-0.10	-0.11	-0.12	-0.05	-0.02
1830 nm reflectance	-0.04	-0.11	-0.10	-0.09	-0.11	-0.12	-0.04	-0.02
Difference1[d]	0.06	-0.09	0.08	0.03	-0.15	0.01	0.17	0.06
Difference2[d]	0.11	-0.40	-0.04	-0.08	-0.29	-0.03	0.20	0.11
Difference3[d]	-0.10	0.46	0.12	0.07	0.22	0.05	-0.10	-0.09
Difference4[d]	0.14	-0.49	-0.18	-0.18	-0.27	-0.05	0.13	0.09
Difference5[d]	-0.12	0.48	0.13	0.13	0.24	0.07	-0.09	-0.09
Difference6[d]	0.05	-0.46	-0.23	-0.09	-0.17	0.06	0.18	0.08
Difference7[d]	0.06	0.40	0.21	0.01	0.02	-0.11	-0.16	-0.04
Difference8[d]	0.02	0.36	0.46	0.32	-0.00	-0.06	-0.04	0.03
Difference9[d]	-0.06	0.42	0.11	0.01	0.17	-0.03	-0.18	-0.08
Difference10[d]	0.05	-0.14	0.09	0.14	-0.11	0.12	0.16	0.10
Difference11[d]	-0.11	0.28	0.00	-0.03	0.25	0.05	-0.14	-0.12
Difference12[d]	0.10	-0.16	-0.04	-0.06	-0.21	-0.12	0.01	0.09
Difference13[d]	-0.10	0.28	0.13	0.10	0.19	0.06	-0.04	-0.10
Difference14[d]	-0.07	-0.16	-0.12	-0.12	-0.01	0.06	-0.02	-0.01

[a] P -values greater than r = 0.09 are significant ($P < 0.05$).
[b] P -values greater than r = 0.12 are significant ($P < 0.05$).
[c] P -values greater than r = 0.11 are significant ($P < 0.05$).
[d] These represent slope calculations of reflectance values between two wavelength measurements. Difference1 = 350nm reflectance -404nm reflectance; Difference2 = 404nm reflectance -512nm reflectance; Difference3 = 512nm reflectance -542nm reflectance; Difference4 = 542nm reflectance -562nm reflectance; Difference5 = 562nm reflectance -577nm reflectance; Difference6 = 577nm reflectance -704nm reflectance; Difference7 = 704nm reflectance -766nm reflectance; Difference8 = 766nm reflectance -792nm reflectance; Difference9 = 792nm reflectance -983nm reflectance; Difference10 = 983nm reflectance -1079nm reflectance; Difference11 = 1079nm reflectance -1193nm reflectance; Difference12 = 1193nm reflectance -1265nm reflectance; Difference13 = 1265nm reflectance -1458nm reflectance; Difference14 = 1458nm reflectance -1830nm reflectance.

Simple correlations within VISIBLE-NIR and difference values are shown in Tables 7 and 8. Simple correlations were high for reflectance values from wavelengths that were in close proximity within the spectrum. However, relationships were weak, or not significant between reflectance values from more distant areas of the spectrum. This is the same for simple correlations between VISIBLE-NIR differences (Tables 9 and 10). The strongest correlations continued to be found in the range of 550 nm reflectance to 930 nm reflectance values. Shackelford et al. (2005) found similar results. Difference values had high correlations to reflectance values that were components of the difference calculations. Reflectance values of 1458 nm, 1830 nm and 350 nm had low correlations with VISIBLE-NIR difference values. Simple correlations within VISIBLE-NIR difference values were similar to the correlations with VISIBLE-NIR reflectance values. Differences 1 and 14 had the lowest correlations within the differences. Since there is such a broad range of the spectrum being used, we can conclude that different information is being obtained from different components of the spectrum.

Table 7
Simple correlations coefficients between independent variables for the calibration data.[a]

Variables	pH	*L**	*a**	*b**	Resistance	Reactance	Phase angle	Partial capacitance
pH								
*L**	0.10							
*a**	-0.04	-0.11						
*b**	-0.20	-0.26	0.79					
Resistance	0.02	0.19	-0.08	0.01				
Reactance	0.06	0.07	-0.09	0.05	0.60			
Phase angle	0.04	-0.29	0.01	0.11	-0.30	0.50		
Partial capacitance	0.02	-0.22	0.05	0.01	-0.90	-0.25	0.60	
350 nm reflectance	0.05	-0.12	0.00	-0.01	-0.22	-0.03	0.20	0.25
404 nm reflectance	-0.02	-0.10	-0.10	-0.10	-0.20	-0.05	0.12	0.21
512 nm reflectance	-0.15	0.14	-0.07	-0.02	0.10	0.01	-0.14	-0.13
542 nm reflectance	-0.12	0.02	-0.12	-0.07	0.02	-0.01	-0.09	-0.04
562 nm reflectance	-0.14	0.07	-0.09	-0.04	0.07	0.00	-0.12	-0.09
577 nm reflectance	-0.13	0.03	-0.12	-0.06	0.03	-0.01	-0.10	-0.05
704 nm reflectance	-0.20	0.26	0.13	0.12	0.17	0.00	-0.22	-0.22
766 nm reflectance	-0.20	0.25	0.11	0.12	0.18	0.01	-0.21	-0.23
792 nm reflectance	-0.19	0.23	0.04	0.06	0.18	0.01	-0.22	-0.23
983 nm reflectance	-0.15	0.12	-0.02	0.02	0.13	0.04	-0.14	-0.16
1079 nm reflectance	-0.16	0.16	-0.04	0.01	0.15	0.03	-0.17	-0.19
1193 nm reflectance	-0.15	0.03	-0.05	-0.02	-0.01	-0.04	-0.09	-0.01
1265 nm reflectance	-0.13	0.07	-0.03	-0.00	0.04	-0.01	-0.10	-0.05
1458 nm reflectance	-0.10	-0.06	-0.12	-0.11	-0.12	-0.10	-0.04	0.10
1830 nm reflectance	-0.10	-0.05	-0.11	-0.10	-0.11	-0.09	-0.04	0.09
Difference1[b]	0.10	-0.12	0.08	0.06	-0.19	-0.01	0.21	0.23
Difference2[b]	0.15	-0.38	-0.05	-0.13	-0.34	-0.06	0.29	0.38
Difference3[b]	-0.15	0.41	0.12	0.16	0.25	-0.05	-0.21	-0.29
Difference4[b]	0.18	-0.43	-0.20	-0.29	-0.30	-0.07	0.23	0.34
Difference5[b]	-0.15	0.41	0.14	0.22	0.28	-0.08	-0.20	-0.31
Difference6[b]	0.20	-0.36	-0.29	-0.23	-0.22	-0.01	0.23	0.27
Difference7[b]	-0.17	0.27	0.27	0.11	0.10	-0.06	-0.20	-0.15
Difference8[b]	-0.17	0.23	0.61	0.53	0.05	-0.01	-0.06	-0.05
Difference9[b]	-0.20	0.32	0.12	0.10	0.20	-0.02	-0.26	-0.27
Difference10[b]	0.11	-0.21	0.08	0.07	-0.16	-0.00	0.19	0.20
Difference11[b]	-0.10	0.29	-0.00	0.05	0.32	0.11	-0.22	-0.35
Difference12[b]	-0.03	-0.22	-0.08	-0.11	-0.27	-0.15	0.10	0.25
Difference13[b]	-0.09	0.27	0.18	0.22	0.27	0.14	-0.12	-0.27
Difference14[b]	-0.04	-0.14	-0.13	-0.13	-0.09	-0.06	-0.02	0.05

[a] *P* -values greater than r = 0.10 are significant ($P < 0.05$).

[b] These represent slope calculations of reflectance values between two wavelength measurements. Difference1 = 350nm reflectance -404nm reflectance; Difference2 = 404nm reflectance -512nm reflectance; Difference3 = 512nm reflectance -542nm reflectance; Difference4 = 542nm reflectance -562nm reflectance; Difference5 = 562nm reflectance -577nm reflectance; Difference6 = 577nm reflectance -704nm reflectance; Difference7 = 704nm reflectance -766nm reflectance; Difference8 = 766nm reflectance -792nm reflectance; Difference9 = 792nm reflectance -983nm reflectance; Difference10 = 983nm reflectance -1079nm reflectance; Difference11 = 1079nm reflectance -1193nm reflectance; Difference12 = 1193nm reflectance -1265nm reflectance; Difference13 = 1265nm reflectance -1458nm reflectance; Difference14 = 1458nm reflectance -1830nm reflectance.

Table 8
Simple correlation coefficients between VISIBLE-NIR reflectance values and difference variables for prediction data.[a]

Variable	350 nm	404 nm	512 nm	542 nm	562 nm	577 nm	704 nm	766 nm	792 nm	983 nm	1079 nm	1193 nm	1265 nm	1458 nm	1830 nm
404 nm reflectance	0.86														
512 nm reflectance	0.36	0.66													
542 nm reflectance	0.39	0.73	0.96												
562 nm reflectance	0.36	0.68	0.99	0.99											
577 nm reflectance	0.38	0.71	0.96	1.00	0.99										
704 nm reflectance	0.18	0.41	0.86	0.74	0.80	0.74									
766 nm reflectance	0.20	0.43	0.89	0.76	0.82	0.77	0.99								
792 nm reflectance	0.21	0.45	0.89	0.78	0.84	0.78	0.98	0.99							
983 nm reflectance	0.31	0.58	0.92	0.90	0.92	0.90	0.86	0.90	0.91						
1079 nm reflectance	0.20	0.46	0.86	0.82	0.85	0.82	0.86	0.89	0.91	0.97					
1193 nm reflectance	0.27	0.59	0.84	0.90	0.89	0.91	0.67	0.71	0.72	0.90	0.88				
1265 nm reflectance	0.24	0.54	0.83	0.88	0.87	0.89	0.68	0.72	0.73	0.92	0.90	0.99			
1458 nm reflectance	0.34	0.67	0.75	0.88	0.83	0.88	0.48	0.51	0.52	0.72	0.65	0.91	0.86		
1830 nm reflectance	0.32	0.63	0.73	0.85	0.81	0.86	0.46	0.49	0.50	0.71	0.65	0.92	0.86	0.99	
Difference1[b]	0.93	0.60	0.07	0.08	0.05	0.06	-0.02	-0.01	-0.00	0.06	-0.02	-0.01	-0.02	0.04	0.03
Difference2[b]	0.73	0.59	-0.23	-0.09	-0.18	-0.11	-0.40	-0.40	-0.39	-0.24	-0.33	-0.14	-0.19	0.06	0.04
Difference3[b]	0.08	0.15	0.62	0.38	0.49	0.38	0.80	0.79	0.78	0.54	0.56	0.25	0.28	0.03	0.02
Difference4[b]	0.14	0.08	-0.54	-0.30	-0.42	-0.30	-0.72	-0.73	-0.70	-0.50	-0.53	-0.24	-0.28	0.01	0.00
Difference5[b]	-0.03	0.02	0.57	0.32	0.44	0.33	0.75	0.74	0.72	0.51	0.53	0.22	0.26	-0.03	-0.03
Difference6[b]	0.02	-0.06	-0.52	-0.31	-0.40	-0.31	-0.87	-0.84	-0.82	-0.56	-0.61	-0.29	-0.31	-0.03	-0.02
Difference7[b]	0.02	0.16	0.44	0.30	0.35	0.30	0.73	0.66	0.62	0.34	0.35	0.20	0.18	0.12	0.10
Difference8[b]	-0.10	-0.09	0.08	-0.01	0.04	-0.00	0.27	0.23	0.12	0.02	-0.04	0.01	0.02	-0.04	-0.03
Difference9[b]	-0.00	0.11	0.56	0.36	0.44	0.36	0.84	0.81	0.80	0.48	0.53	0.23	0.21	0.07	0.04
Difference10[b]	0.24	0.15	-0.27	-0.18	-0.23	-0.19	-0.46	-0.48	-0.51	-0.44	-0.64	-0.39	-0.42	-0.15	-0.17
Difference11[b]	0.01	0.07	0.51	0.33	0.41	0.33	0.74	0.75	0.78	0.64	0.73	0.31	0.38	-0.01	-0.02
Difference12[b]	0.10	0.10	-0.18	-0.14	-0.18	-0.14	-0.22	-0.25	-0.25	-0.39	-0.41	-0.22	-0.38	0.06	0.03
Difference13[b]	-0.15	-0.15	0.25	0.12	0.19	0.12	0.44	0.46	0.46	0.49	0.56	0.26	0.38	-0.15	-0.13
Difference14[b]	0.26	0.36	0.24	0.25	0.23	0.24	0.22	0.20	0.23	0.11	0.06	-0.03	-0.08	0.04	-0.05

[a] *P* -values greater than r = 0.08 are significant ($P < 0.05$).

[b] These represent slope calculations of reflectance values between two wavelength measurements. Difference1 = 350nm reflectance -404nm reflectance; Difference2 = 404nm reflectance -512nm reflectance; Difference3 = 512nm reflectance -542nm reflectance; Difference4 = 542nm reflectance -562nm reflectance; Difference5 = 562nm reflectance -577nm reflectance; Difference6 = 577nm reflectance -704nm reflectance; Difference7 = 704nm reflectance -766nm reflectance; Difference8 = 766nm reflectance -792nm reflectance; Difference9 = 792nm reflectance -983nm reflectance; Difference10 = 983nm reflectance -1079nm reflectance; Difference11 = 1079nm reflectance -1193nm reflectance; Difference12 = 1193nm reflectance -1265nm reflectance; Difference13 = 1265nm reflectance -1458nm reflectance; Difference14 = 1458nm reflectance -1830nm reflectance.

Table 9
Simple correlation coefficients between VISIBLE-NIR reflectance values and difference variables for calibration data.[a]

Variable	350 nm	404 nm	512 nm	542 nm	562 nm	577 nm	704 nm	766 nm	792 nm	983 nm	1079 nm	1193 nm	1265 nm	1458 nm	1830 nm
404 nm reflectance	0.84														
512 nm reflectance	0.36	0.70													
542 nm reflectance	0.39	0.76	0.96												
562 nm reflectance	0.36	0.72	0.99	0.99											
577 nm reflectance	0.38	0.75	0.96	1.00	0.99										
704 nm reflectance	0.19	0.46	0.87	0.75	0.81	0.75									
766 nm reflectance	0.20	0.48	0.89	0.78	0.83	0.78	0.99								
792 nm reflectance	0.21	0.50	0.90	0.80	0.85	0.80	0.99	0.99							
983 nm reflectance	0.32	0.64	0.93	0.90	0.92	0.90	0.88	0.91	0.92						
1079 nm reflectance	0.20	0.52	0.87	0.82	0.85	0.83	0.88	0.91	0.93	0.97					
1193 nm reflectance	0.28	0.65	0.85	0.90	0.89	0.91	0.72	0.75	0.76	0.91	0.89				
1265 nm reflectance	0.25	0.60	0.84	0.88	0.88	0.89	0.72	0.76	0.77	0.93	0.91	0.98			
1458 nm reflectance	0.35	0.71	0.77	0.89	0.85	0.89	0.54	0.56	0.58	0.74	0.68	0.92	0.86		
1830 nm reflectance	0.33	0.69	0.76	0.87	0.83	0.88	0.52	0.55	0.57	0.74	0.69	0.92	0.87	0.99	
Difference1[b]	0.91	0.55	0.03	0.03	0.01	0.02	-0.08	-0.06	-0.06	0.01	-0.08	-0.05	-0.06	0.00	-0.00
Difference2[b]	0.70	0.50	-0.27	-0.14	-0.22	-0.15	-0.43	-0.42	-0.41	-0.26	-0.35	-0.16	-0.21	-0.02	0.01
Difference3[b]	0.11	0.20	0.64	0.41	0.51	0.41	0.80	0.79	0.77	0.57	0.59	0.30	0.34	0.08	0.08
Difference4[b]	0.08	0.00	0.56	-0.33	-0.44	-0.33	-0.73	-0.73	-0.70	-0.52	-0.56	-0.28	-0.34	-0.03	-0.04
Difference5[b]	0.03	0.11	0.61	0.37	0.48	0.37	0.75	0.75	0.73	0.55	0.57	0.28	0.33	0.04	0.04
Difference6[b]	0.03	-.10	-0.52	-0.32	-0.41	-0.33	-0.87	-0.84	-0.81	-0.58	-0.64	-0.34	-0.37	-0.09	-0.09
Difference7[b]	0.00	0.19	0.50	0.36	0.41	0.36	0.77	0.72	0.68	0.43	0.44	0.30	0.28	0.20	0.18
Difference8[b]	-0.05	-0.04	0.17	0.07	0.13	0.08	0.40	0.36	0.26	0.16	0.11	0.12	0.14	0.01	0.02
Difference9[b]	-0.02	0.15	0.58	0.39	0.47	0.39	0.84	0.81	0.81	0.51	0.57	0.29	0.28	0.15	0.13
Difference10[b]	0.33	0.20	-0.16	-0.08	-0.12	-0.09	-0.40	-0.41	-0.44	-0.34	-0.55	-0.31	-0.34	-0.09	-0.11
Difference11[b]	-0.01	0.11	0.52	0.35	0.43	0.35	0.74	0.75	0.77	0.65	0.74	0.34	0.42	0.05	0.04
Difference12[b]	0.08	0.05	-0.24	-0.18	-0.23	-0.19	-0.27	-0.30	-0.29	-0.42	-0.43	-0.24	-0.41	0.02	-0.01
Difference13[b]	-0.12	-0.07	0.29	0.16	0.23	0.18	0.48	0.50	0.48	0.52	0.58	0.31	0.44	-0.08	-0.05
Difference14[b]	0.27	0.47	0.39	0.46	0.42	0.45	0.30	0.29	0.32	0.26	0.20	0.22	0.15	0.36	0.28

[a] *P* -values greater than r = 0.08 are significant ($P < 0.05$).

[b] These represent slope calculations of reflectance values between two wavelength measurements. Difference1 = 350nm reflectance -404nm reflectance; Difference2 = 404nm reflectance -512nm reflectance; Difference3 = 512nm reflectance -542nm reflectance; Difference4 = 542nm reflectance -562nm reflectance; Difference5 = 562nm reflectance -577nm reflectance; Difference6 = 577nm reflectance -704nm reflectance; Difference7 = 704nm reflectance -766nm reflectance; Difference8 = 766nm reflectance -792nm reflectance; Difference9 = 792nm reflectance -983nm reflectance; Difference10 = 983nm reflectance -1079nm reflectance; Difference11 = 1079nm reflectance -1193nm reflectance; Difference12 = 1193nm reflectance -1265nm reflectance; Difference13 = 1265nm reflectance -1458nm reflectance; Difference14 = 1458nm reflectance -1830nm reflectance.

Table 10
Simple correlations coefficients between VISIBLE-NIR difference variables for prediction data.

Variables	Difference1	Difference2	Difference3	Difference4	Difference5	Difference6	Difference7	Difference8	Difference9	Difference10	Difference11	Difference12	Difference13
Difference2[b]	0.71												
Difference3[b]	0.01	-0.48											
Difference4[b]	0.16	0.68	-0.94										
Difference5[b]	-0.07	-0.58	0.98	-0.98									
Difference6[b]	0.07	0.48	-0.85	0.80	-0.81								
Difference7[b]	-0.08	-0.27	0.61	-0.49	0.54	-0.81							
Difference8[b]	-0.09	-0.20	0.28	-0.37	0.33	-0.39	0.52						
Difference9[b]	-0.09	-0.47	0.86	-0.76	0.80	-0.92	0.81	0.23					
Difference10[b]	0.26	0.48	-0.37	0.40	-0.37	0.51	-0.22	0.24	-0.45				
Difference11[b]	-0.03	-0.46	0.76	-0.71	0.74	-0.80	0.41	-0.10	0.73	-0.70			
Difference12[b]	0.08	0.33	-0.22	0.33	-0.30	0.21	0.08	-0.06	0.03	0.29	-0.50		
Difference13[b]	-0.12	-0.46	0.48	-0.57	0.55	-0.53	0.12	0.12	0.27	-0.54	0.74	-0.82	
Difference14[b]	0.15	0.20	0.10	0.10	0.00	-0.14	0.29	-0.18	0.32	0.12	0.17	0.26	-0.22

[a] P -values greater than r = 0.08 are significant ($P < 0.05$).

b These represent slope calculations of reflectance values between two wavelength measurements. Difference1 = 350nm reflectance -404nm reflectance; Difference2 = 404nm reflectance -512nm reflectance; Difference3 = 512nm reflectance -542nm reflectance; Difference4 = 542nm reflectance -562nm reflectance; Difference5 = 562nm reflectance -577nm reflectance; Difference6 = 577nm reflectance -704nm reflectance; Difference7 = 704nm reflectance -766nm reflectance; Difference8 = 766nm reflectance -792nm reflectance; Difference9 = 792nm reflectance -983nm reflectance; Difference10 = 983nm reflectance -1079nm reflectance; Difference11 = 1079nm reflectance -1193nm reflectance; Difference12 = 1193nm reflectance -1265nm reflectance; Difference13 = 1265nm reflectance -1458nm reflectance; Difference14 = 1458nm reflectance -1830nm reflectance.

Table 11

Simple correlations coefficients between VISIBLE-NIR difference variables for calibration data.[a]

Variables	Difference1	Difference2	Difference3	Difference 4	Difference5	Difference6	Difference7	Difference8	Difference9	Difference10	Difference11	Difference12	Difference13
Difference2[b]	0.70												
Difference3[b]	0.02	-0.51											
Difference4[b]	0.12	0.67	-0.95										
Difference5[b]	-0.03	-0.59	0.98	-0.98									
Difference6[b]	0.12	0.50	-0.83	0.79	-0.80								
Difference7[b]	-0.14	-0.34	0.64	-0.53	0.57	-0.84							
Difference8[b]	-0.05	-0.26	0.39	-0.47	0.42	-0.51	0.58						
Difference9[b]	-0.15	-0.50	0.84	-0.75	0.78	-0.92	0.84	0.33					
Difference10[b]	0.36	0.46	-0.33	0.36	-0.33	0.52	-0.25	0.11	0.45				
Difference11[b]	-0.09	-0.48	0.75	-0.73	0.75	-0.80	0.46	0.06	0.72	-0.65			
Difference12[b]	0.09	0.35	-0.30	0.42	-0.39	0.25	0.02	-0.15	-0.01	0.24	-0.54		
Difference13[b]	-0.12	-0.45	0.52	-0.61	0.58	-0.56	0.20	0.26	0.28	-0.50	0.74	-0.83	
Difference14[b]	0.05	0.16	0.03	0.14	-0.05	-0.09	0.29	-0.13	0.30	0.15	0.08	0.33	-0.34

[a] *P*-values greater than r = 0.08 are significant ($P < 0.05$).

b These represent slope calculations of reflectance values between two wavelength measurements. Difference1 = 350nm reflectance -404nm reflectance; Difference2 = 404nm reflectance -512nm reflectance; Difference3 = 512nm reflectance -542nm reflectance; Difference4 = 542nm reflectance -562nm reflectance; Difference5 = 562nm reflectance -577nm reflectance; Difference6 = 577nm reflectance -704nm reflectance; Difference7 = 704nm reflectance -766nm reflectance; Difference8 = 766nm reflectance -792nm reflectance; Difference9 = 792nm reflectance -983nm reflectance; Difference10 = 983nm reflectance -1079nm reflectance; Difference11 = 1079nm reflectance -1193nm reflectance; Difference12 = 1193nm reflectance -1265nm reflectance; Difference13 = 1265nm reflectance -1458nm reflectance; Difference14 = 1458nm reflectance -1830nm reflectance.

Table 12
Simple correlation coefficients between dependent and independent variables for prediction data.

Variables	Warner-Bratzler shear force, 1 d, N	Warner-Bratzler shear force, 7 d, N	Warner-Bratzler shear force, 14 d, N	Slice shear force, 1 d, N	Slice shear force ,7 d, N	Slice shear force, 14 d, N
pH[a]	0.18	0.25	0.23	0.25	0.24	0.23
*L**[a]	-0.05	-0.16	-0.11	-0.25	-0.27	-0.27
*a**[a]	-0.24	-0.31	-0.24	-0.31	-0.26	-0.31
*b**[a]	-0.17	-0.26	-0.23	-0.21	-0.15	-0.22
Resistance[a]	-0.00	-0.03	-0.13	-0.04	-0.13	-0.09
Reactance[a]	0.12	0.08	-0.02	0.13	-0.01	0.03
Phase angle[a]	0.10	0.14	0.11	0.19	0.11	0.09
Partial capacitance[a]	0.03	0.08	0.08	0.03	0.11	0.05
350 nm[b]	-0.02	-0.05	-0.14	0.19	0.18	0.24
404 nm[b]	-0.01	-0.02	-0.12	0.22	0.24	0.29
512 nm[b]	-0.11	-0.12	-0.17	0.05	0.09	0.14
542 nm[b]	-0.05	-0.03	-0.11	0.14	0.18	0.22
562 nm[b]	-0.08	-0.07	-0.14	0.10	0.13	0.18
577 nm[b]	-0.06	-0.03	-0.11	0.14	0.17	0.21
704 nm[b]	-0.16	-0.22	-0.24	-0.07	0.03	0.02
766 nm[b]	-0.16	-0.21	-0.24	-0.06	-0.03	0.02
792 nm[b]	-0.16	-0.20	-0.23	-0.03	0.00	0.06
983 nm[b]	-0.13	-0.13	-0.17	0.01	0.04	0.08
1079 nm[b]	-0.13	-0.13	-0.16	0.00	0.03	0.08
1193 nm[b]	-0.07	-0.03	-0.07	0.08	0.14	0.15
1265 nm[b]	-0.09	-0.04	-0.08	0.04	0.09	0.10
1458 nm[b]	-0.01	0.05	-0.03	0.20	0.26	0.27
1830 nm[b]	-0.02	0.05	-0.03	0.19	0.25	0.25
Difference1[bc]	-0.02	-0.07	-0.13	0.14	0.11	0.16
Difference2[bc]	0.10	0.10	0.03	0.22	0.21	0.23
Difference3[bc]	-0.20	-0.29	-0.25	-0.22	-0.21	-0.15
Difference4[bc]	0.20	0.29	-0.22	0.28	0.28	0.25
Difference5[bc]	-0.18	-0.28	-0.23	-0.24	-0.24	-0.20
Difference6[bc]	0.18	0.28	0.25	0.20	-0.17	0.12
Difference7[bc]	-0.09	-0.16	-0.15	-0.08	-0.02	0.01
Difference8[bc]	-0.15	-0.16	-0.10	-0.34	-0.28	-0.34
Difference9[bc]	-0.13	-0.24	-0.24	-0.08	-0.06	0.01
Difference10[bc]	0.06	0.07	0.03	-0.02	0.01	-0.03
Difference11[bc]	-0.14	-0.21	-0.20	-0.11	-0.13	-0.06
Difference12[bc]	0.10	0.08	0.03	0.22	0.23	0.25
Difference13[bc]	-0.15	-0.17	-0.10	-0.29	-0.30	-0.30
Difference14[bc]	0.05	0.03	-0.08	0.17	0.18	0.22

[a] P-values greater than r = 0.10 are significant (P<0.05)
[b] P-values greater than r = 0.09 are significant (P<0.05)
[c] These represent slope calculations of reflectance values between two wavelength measurements. Difference1 = 350nm-404nm; Difference2 = 404nm-512nm; Difference3 = 512nm-542nm; Difference4 = 542nm-562nm; Difference5 = 562nm-577nm; Difference6 = 577nm-704nm; Difference7 = 704nm-766nm; Difference8 = 766nm-792nm; Difference9 = 792nm-983nm; Difference10 = 983nm-1079nm; Difference11 = 1079nm-1193nm; Difference12 = 1193nm-1265nm; Difference13 = 1265nm-1458nm; Difference14 = 1458nm-1830nm

Table 13
Simple correlation coefficients between dependent and independent variables for calibration data.

Variables	Warner-Bratzler shear force, 1 d, N	Warner-Bratzler shear force, 7 d, N	Warner-Bratzler shear force, 14 d, N	Slice shear force ,1 d, N	Slice shear force ,7 d, N	Slice shear force, 14 d, N
pH[a]	0.21	0.25	0.15	0.26	0.18	0.22
*L**[a]	-0.01	-0.05	0.07	-0.14	-0.22	-0.16
*a**[a]	-0.31	-0.34	-0.23	-0.35	-0.28	-0.34
*b**[a]	-0.38	-0.41	-0.32	-0.35	-0.33	-0.39
Resistance[a]	-0.08	-0.15	-0.12	-0.14	-0.17	-0.19
Reactance[a]	0.15	0.05	0.02	0.09	0.02	-0.01
Phase angle[a]	0.24	0.17	0.12	0.25	0.19	0.16
Partial capacitance[a]	0.18	0.21	0.18	0.21	0.23	0.23
350 nm reflectance [b]	-0.02	-0.04	-0.10	0.19	0.23	0.91
404 nm reflectance [b]	-0.01	-0.03	-0.11	0.20	0.27	0.55
512 nm reflectance [b]	-0.10	-0.13	-0.12	0.03	0.14	0.03
542 nm reflectance [b]	-0.04	-0.05	-0.09	0.12	0.21	0.03
562 nm reflectance [b]	-0.07	-0.09	-0.10	0.08	0.17	0.01
577 nm reflectance [b]	-0.05	-0.06	-0.09	0.11	0.20	0.02
704 nm reflectance [b]	-0.18	-0.23	-0.16	-0.08	0.04	-0.08
766 nm reflectance [b]	-0.17	-0.23	-0.16	-0.07	0.04	-0.06
792 nm reflectance [b]	-0.15	-0.22	-0.15	-0.04	0.07	-0.06
983 nm reflectance [b]	-0.09	-0.13	-0.11	0.01	0.10	0.01
1079 nm reflectance [b]	-0.07	-0.13	-0.10	0.01	0.09	-0.08
1193 nm reflectance [b]	-0.01	-0.02	-0.07	0.09	0.08	-0.05
1265 nm reflectance [b]	-0.01	-0.03	-0.06	0.06	0.05	-0.06
1458 nm reflectance [b]	0.03	0.04	-0.07	0.20	0.20	0.00
1830 nm reflectance [b]	0.04	0.05	-0.06	0.20	0.19	-0.00
Difference1[bc]	-0.02	-0.03	-0.08	0.14	0.10	0.16
Difference2[bc]	0.11	0.11	0.00	0.23	0.23	0.20
Difference3[bc]	-0.23	-0.27	-0.15	-0.22	-0.22	-0.12
Difference4[bc]	0.22	0.26	0.14	0.26	0.29	0.22
Difference5\[bc]	-0.21	-0.26	-0.14	-0.23	-0.25	-0.16
Difference6 [bc]	0.22	0.29	0.16	0.20	0.17	0.10
Difference7 [bc]	-0.17	-0.20	-0.12	-0.10	-0.01	0.02
Difference8 [bc]	-0.21	-0.19	-0.12	-0.29	-0.22	-0.30
Difference9 [bc]	-0.21	-0.28	-0.17	-0.11	-0.10	0.01
Difference10 [bc]	-0.03	0.06	0.02	0.01	-0.08	0.02
Difference11 [bc]	-0.13	-0.23	-0.11	-0.12	-0.15	-0.04
Difference12 [bc]	-0.01	0.04	-0.03	0.12	0.16	0.17
Difference13 [bc]	-0.07	-0.13	0.01	-0.23	-0.25	-0.21
Difference14 [bc]	-0.09	-0.13	-0.11	0.06	0.15	0.21

[a] *P* -values greater than r = 0.11 are significant ($P < 0.05$).
[b] *P* -values greater than r = 0.09 are significant ($P < 0.05$).
[c] These represent slope calculations of reflectance values between two wavelength measurements. Difference1 = 350nm reflectance -404nm reflectance; Difference2 = 404nm reflectance -512nm reflectance; Difference3 = 512nm reflectance -542nm reflectance; Difference4 = 542nm reflectance -562nm reflectance; Difference5 = 562nm reflectance -577nm reflectance; Difference6 = 577nm reflectance -704nm reflectance; Difference7 = 704nm reflectance -766nm reflectance; Difference8 = 766nm reflectance -792nm reflectance; Difference9 = 792nm reflectance -983nm reflectance; Difference10 = 983nm reflectance -1079nm reflectance; Difference11 = 1079nm reflectance -1193nm reflectance; Difference12 = 1193nm reflectance -1265nm reflectance; Difference13 = 1265nm reflectance -1458nm reflectance; Difference14 = 1458nm reflectance -1830nm reflectance.

Simple correlations between independent and dependent variables were reported in Tables 12 and 13. Slice shear force values had higher correlations with independent variables than Warner-Bratzler shear force values. Shackelford et al. (1999a) reported that the cause of lower correlations for Warner-Bratzler shear force was due to variability in Warner-Bratzler shear force values. Slice shear is more simple to conduct and has fewer steps that could cause variation in procedure when compared to Warner-Bratzler shear force (Shackelford et al., 1999a). Electrical impedance values showed weak or no relationship to the dependent variables. This was similar to the results reported by Wulf and Page (2000). pH had a higher correlation values with Warner-Bratzler and Slice shear force values (0.18 to 0.25, respectively). L^*, a^* and b^* color space values had higher correlations with 7 and 14 d Warner-Bratzler shear force values than 1 d Warner-Bratzler shear force values. Differences 2, 3, 4, 5, 6, 8, and 11, 12, 13 and 14 had higher correlations to Slice shear force values than others. Some differences (9, 12, and 14) were significant or strongly correlated for one method of shear force, but not the other. VISIBLE-NIR reflectance values had lower correlations than the difference values. Fourteen d Slice shear force values had the highest correlations (0.24 to 0.29) with VISIBLE-NIR reflectance values compared to 1 and 7 d Slice shear force values. The reflectance values at the exterior of the spectrum (350nm reflectance, 404 nm reflectance, 1458nm reflectance and 1830nm reflectance) had a stronger correlation than the middle of the spectrum to Slice shear force values. For Warner-Bratzler shear force values, the opposite was true. There were higher correlations (-0.16 to -0.24)

reported for wavelengths in the mid-range reflectance values for Warner-Bratzler shear force than those with Slice shear force values.

With the values found, pH, color space values, and difference values should have predictive values for Warner-Bratzler and Slice shear force values. The stronger correlations with these variables will most likely contribute to prediction of beef tenderness.

Stepwise regression equations are found in the tables on pages 39 through 46. Stepwise regression was used to understand variables for prediction of Warner-Bratzler and Slice shear force values at the three aging times. Regression equations were generated using multiple strategies. The first strategy was to utilize only VISIBLE-NIR to predict tenderness. Second, the use of pH, color space values and VISIBLE-NIR variables were available to enter into the stepwise regression models. This strategy was used to see if prediction could be improved by using more than one technology. The third strategy was to add electrical impedance into the equation. pH and color were used alone to see if the equation would be strong when excluding VISIBLE-NIR. The same process was done with electrical impedance. When all independent variables were added into the equation (Table 13), R^2 values were high (0.17 to 0.38). Difference 6 (577 nm reflectance to 704 nm reflectance) contributed the most to the equations predicting 14 d Warner-Bratzler shear forces. In addition to 1, 7, and 14 d Slice shear force values, Warner-Bratzler shear force equations had R^2 values of 0.17 to 0.38, while Slice shear force equations had R^2 values of 0.34 to 0.29. However, lower R^2 values were found for Slice shear force values compared to Warner-Bratzler shear force.

Table 14
Stepwise regression using pH, *L**, *a**, *b** color space values, resistance, reactance, phase angle, partial capacitance, VISIBLE-NIR and difference variables to predict Warner-Bratzler shear forces for 1, 7, and 14 day and Slice shear forces for 1, 7, and 14 day.

Dependent variable	Intercept	β-value	Independent variable	Partial R^2	R^2
Warner-Bratzler shear force, 1 d	-32.22	18.44	pH	0.01	0.17
		-0.39	a*	0.01	
		0.27	Reactance	0.03	
		112.35	512 nm reflectance	0.02	
		-130.72	792 nm reflectance	0.09	
Warner-Bratzler shear force, 7 d	-111.01	34.50	pH	0.06	0.38
		-0.70	a*	0.06	
		219.91	562 nm reflectance	0.01	
		-181.28	792 nm reflectance	0.01	
		-37.29	Difference2[a]	0.01	
		6.89	Difference6 [a]	0.22	
		697.86	Difference12 [a]	0.01	
		259.17	Difference13 [a]	0.01	
Warner-Bratzler shear force, 14 d	-52.34	20.29	pH	0.07	0.35
		-0.44	b*	0.03	
		0.00	partial capacitance	0.00	
		-36.37	Difference2 [a]	0.01	
		97.36	Difference6 [a]	0.22	
		185.28	Difference8 [a]	0.02	
Slice shear force, 1 d	-415.45	165.03	pH	0.02	0.34
		1.67	Reactance	0.02	
		3937.90	562 nm reflectance	0.01	
		-3647.34	704 nm reflectance	0.01	
		-2407.73	Difference6 [a]	0.27	
		1594.14	Difference12 [a]	0.01	
Slice shear force, 7 d	-366.54	126.46	pH	0.03	0.29
		659.45	Difference6 [a]	0.25	
		-566.07	Difference10 [a]	0.01	
Slice shear force, 14 d	-137.41	75.55	pH	0.02	0.29
		-190.90	Difference2 [a]	0.01	
		531.23	Difference6 [a]	0.25	
		392.01	Difference10 [a]	0.01	

[a] These represent slope calculations of reflectance values between two wavelength measurements. Difference1 = 350nm reflectance -404nm reflectance; Difference2 = 404nm reflectance -512nm reflectance; Difference3 = 512nm reflectance -542nm reflectance; Difference4 = 542nm reflectance -562nm reflectance; Difference5 = 562nm reflectance -577nm reflectance; Difference6 = 577nm reflectance -704nm reflectance; Difference7 = 704nm reflectance -766nm reflectance; Difference8 = 766nm reflectance -792nm reflectance; Difference9 = 792nm reflectance -983nm reflectance; Difference10 = 983nm reflectance -1079nm reflectance; Difference11 = 1079nm reflectance -1193nm reflectance; Difference12 = 1193nm reflectance -1265nm reflectance; Difference13 = 1265nm reflectance -1458nm reflectance; Difference14 = 1458nm reflectance -1830nm reflectance.

In Table 15, equations using VISIBLE-NIR reflectance values and differences values were reported. For Warner-Bratzler shear force values, R^2 values of 0.06 to 0.14 were found. Higher R^2 values were found for Slice shear equations (0.34 to 0.36). This would be expected as Slice shear force values had stronger simple correlation coefficients to VISIBLE-NIR independent variables. Difference values 3, 7, and 8 contributed to the Slice shear force equations with difference 8 values contributing the most in all three of the Slice shear force equations. These R^2 values were lower than those reported by other studies (Andrés, Silva, Soares-Pereira, Martins, Bruno-Soares &

Murray, 2008; Park et al., 1998; Yancey, Apple, Meullenet & Sawyer, 2010) that reported R^2 values of 0.63 to 0.79. However, these numbers are similar to what Shackelford et al. (2005) reported for R^2 values predicting tenderness (0.38 and 0.22). Our R^2 values were higher than those reported by Nath (2008). This can be due to a larger n in our study and the use of different NIR instruments.

In our study, pH, L^*, a^* and b^* color space values, and electrical impedance were used alone and together in prediction equations. Electrical impedance had the lowest predictability with R^2 values of 0.01 to 0.03. This is comparable to what Wulf and Page (2000) reported. Wulf and Page (2000) found electrical impedance to have little to no relation to predicting beef tenderness. There were no regression models reported by Wulf and Page (2000) using electrical impedance. Nath (2008) reported a low R^2 value with electrical impedance (0.05). However, Nath (2008) predicted the very tender steaks using electrical impedance and NIR. Nath (2008) attributed the ability to predict the very tender steaks to the electrical impedance readings. Nath (2008) penetrated the muscle 5 cm with the electrical impedance whereas, in our study electrical impedance was placed on the 12^{th} rib lean surface. Based on our regression equations and results by Wulf and Page (2000) and Nath (2008), electrical impedance was not an effective tool for predicting tough steaks.

Table 15
Stepwise regression using VISIBLE-NIR and difference variables to predict Warner-Bratzler shear forces for 1, 7, and 14 day and Slice shear forces for 1, 7, and 14 day

Dependent variable	Intercept	β-value	Independent variable	Partial R^2	R^2
Warner-Bratzler shea forcer, 1 d	40.44	84.95	Difference6 [a]	.01	0.06
		390.27	Difference7 [a]	.01	
		-295.08	Difference8 [a]	.01	
Warner-Bratzler shear force, 7 d	38.53	-9.16	350 nm reflectance	0.00	0.14
		70.23	542 nm reflectance	0.01	
		-34.05	983 nm reflectance	0.01	
		799.59	Difference3 [a]	0.01	
		1604.78	Difference4 [a]	0.01	
		3116.16	Difference5 [a]	0.01	
		126.54	Difference7 [a]	0.01	
		-164.00	Difference8 [a]	0.01	
Warner-Bratzler shear force, 14 d	35.34	-10.09	Difference1 [a]	0.02	0.12
		100.94	Difference6 [a]	0.01	
		297.26	Difference7 [a]	0.01	
		-86.18	Difference10 [a]	0.02	
		43.06	Difference13 [a]	0.01	
Slice shear force, 1 d	28.50	23542.00	542 nm reflectance	0.03	0.34
		37168.00	562 nm reflectance	0.04	
		-60038.00	577 nm reflectance	0.01	
		249.00	Difference1 [a]	0.02	
		-18398.00	Difference3 [a]	0.01	
		2479.87	Difference7 [a]	0.00	
		-5153.98	Difference8 [a]	0.12	
		1627.39	Difference9 [a]	0.02	
		-1089.86	Difference13 [a]	0.07	
		-5138.66	Difference14 [a]	0.02	
Slice shear force, 7 d	44.37	75.70	350 nm reflectance	0.03	0.31
		-868.96	1079 nm reflectance	0.00	
		1327.42	1265 nm reflectance	0.05	
		-11948.00	Difference3 [a]	0.02	
		16070.00	Difference4 [a]	0.00	
		42814.00	Difference5 [a]	0.02	
		-952.38	Difference6 [a]	0.01	
		1427.48	Difference7 [a]	0.02	
		-5074.23	Difference8 [a]	0.06	
		-1506.92	Difference13 [a]	0.09	
Slice shear force, 14 d	0.25	-421.21	1079 nm reflectance	0.06	0.36
		838.85	1830 nm reflectance	0.01	
		98.68	Difference1 [a]	0.02	
		-9072.46	Difference3 [a]	0.04	
		16069.00	Difference4 [a]	0.02	
		36283.00	Difference5 [a]	0.01	
		-746.87	Difference6 [a]	0.00	
		1166.54	Difference7 [a]	0.02	
		-4209.08	Difference8 [a]	0.11	
		-545.22	Difference13 [a]	0.07	

[a] These represent slope calculations of reflectance values between two wavelength measurements. Difference1 = 350nm reflectance - 404nm reflectance; Difference2 = 404nm reflectance -512nm reflectance; Difference3 = 512nm reflectance -542nm reflectance; Difference4 = 542nm reflectance -562nm reflectance; Difference5 = 562nm reflectance -577nm reflectance; Difference6 = 577nm reflectance -704nm reflectance; Difference7 = 704nm reflectance -766nm reflectance; Difference8 = 766nm reflectance -792nm reflectance; Difference9 = 792nm reflectance -983nm reflectance; Difference10 = 983nm reflectance -1079nm reflectance; Difference11 = 1079nm reflectance -1193nm reflectance; Difference12 = 1193nm reflectance -1265nm reflectance; Difference13 = 1265nm reflectance -1458nm reflectance; Difference14 = 1458nm reflectance -1830nm reflectance.

Using pH and *L**, *a** and *b** color space values to predict Warner-Bratzler shear force and Slice shear force values, higher R^2 values were found (Table 17). Equations to predict Warner-Bratzler shear force values still showed lower R^2 values (0.11 to 0.22) when compared to equations to predict Slice shear force (0.24 to 0.28). When electrical impedance was incorporated into the equation, R^2 values did not increase for Slice shear

force predictability, but equations to predict Warner-Bratzler shear force had higher R^2 values (0.12 to 0.25). Electrical impedance values contributed little predictability to prediction equations, when used alone or in combination with VISIBLE-NIR, pH or color space values.

Table 16
Stepwise regression using pH, *L*, a*, b** color space values, VISIBLE-NIR wavelengths, and differences to predict Warner-Bratzler shear forces 1, 7, and 14 day and Slice shear forces 1, 7, and 14 day.

Dependent variable	Intercept	β-value	Independent variables	Partial R^2	R^2
Warner-Bratzler shear force, 1 d	-72.77	24.12	pH	0.03	0.19
		-0.71	a*	0.03	
		-1753.53	Difference3 [a]	0.01	
		2149.34	Difference4 [a]	0.01	
		5755.24	Difference5 [a]	0.01	
		110.88	Difference9 [a]	0.01	
Warner-Bratzler shear force, 7 d	-106.70	30.10	pH	0.05	0.30
		-0.66	a*	0.06	
		27.37	1193 nm reflectance	0.01	
		-15.15	Difference1 [a]	0.01	
		70.34	Difference6 [a]	0.16	
Warner-Bratzler shear force, 14 d	-57.44	20.18	pH	0.05	0.29
		-0.44	a*	0.04	
		-30.62	Difference2 [a]	0.00	
		-71.56	Difference9 [a]	0.17	
		-66.81	Difference10 [a]	0.01	
		-81.62	Difference11 [a]	0.01	
Slice shear force, 1 d	-1169.42	270.23	pH	0.08	0.42
		-2.26	L*	0.00	
		-4.75	a*	0.02	
		287.26	350 nm reflectance	0.01	
		-15506.00	Difference3 [a]	0.01	
		37702.00	Difference5 [a]	0.02	
		3998.50	Difference7 [a]	0.01	
		-5717.86	Difference8 [a]	0.17	
		-988.13	Difference13 [a]	0.06	
Slice shear force, 7 d	-680.98	170.49	pH	0.03	0.38
		-1.62	L*	0.00	
		-6.29	a*	0.00	
		5.06	b*	0.02	
		-1048.59	1193 nm reflectance	0.01	
		1451.27	1830 nm reflectance	0.03	
		-6769.14	Difference3 [a]	0.02	
		23318.00	Difference4 [a]	0.15	
		36062.00	Difference5 [a]	0.07	
		-569.59	Difference6 [a]	0.01	
		-1430.18	Difference8 [a]	0.02	
Slice shear force, 14 d	-649.80	146.65	pH	0.05	0.44
		-2.00	L*	0.01	
		-4.95	a*	0.02	
		2.77	b*	0.01	
		149.50	350 nm reflectance	0.01	
		-5936.38	Difference 3 [a]	0.01	
		13453.00	Difference5 [a]	0.01	
		3255.98	Difference7 [a]	0.01	
		-3643.74	Difference 8 [a]	0.19	
		-450.11	Difference 13[a]	0.07	

[a] These represent slope calculations of reflectance values between two wavelength measurements. Difference1 = 350nm reflectance -404nm reflectance; Difference2 = 404nm reflectance -512nm reflectance; Difference3 = 512nm reflectance -542nm reflectance; Difference4 = 542nm reflectance -562nm reflectance; Difference5 = 562nm reflectance -577nm reflectance; Difference6 = 577nm reflectance -704nm reflectance; Difference7 = 704nm reflectance -766nm reflectance; Difference8 = 766nm reflectance -792nm reflectance; Difference9 = 792nm reflectance -983nm reflectance; Difference10 = 983nm reflectance -1079nm reflectance; Difference11 = 1079nm reflectance -1193nm reflectance; Difference12 = 1193nm reflectance -1265nm reflectance; Difference13 = 1265nm reflectance -1458nm reflectance; Difference14 = 1458nm reflectance -1830nm reflectance.

Table 17
Stepwise regression using pH and *L*, a*, and b** color space values to predict Warner-Bratzler shear forces for 1, 7, and 14 day and Slice shear forces for 1, 7, and 14 day.

Dependent variable	Intercept	β-value	Independent variable	Partial R^2	R^2
Warner-Bratzler shear force, 1 d	-125.27	7.56	pH	0.04	0.11
		0.32	a*	0.06	
		0.33	b*	0.01	
Warner-Bratzler shear force, 7 d	-116.43	33.65	pH	0.08	0.22
		-0.60	L*	0.04	
		-0.93	a*	0.10	
Warner-Bratzler shear force, 14 d	-85.40	24.04	pH	0.06	0.14
		-0.33	L*	0.02	
		-0.53	a*	0.06	
Slice shear force, 1 d	-1315.51	367.35	pH	0.09	0.28
		-7.63	L*	0.09	
		-13.01	a*	0.10	
		5.10	b*	0.01	
Slice shear force, 7 d	-781.17	232.17	pH	0.08	0.24
		-5.56	L*	0.07	
		-8.53	a*	0.08	
		4.31	b*	0.01	
Slice shear force, 14 d	-628.23	193.61	pH	0.09	0.27
		-4.85	L*	0.08	
		-6.92	a*	0.09	
		2.24	b*	0.01	

pH accounted for variation in all regression equations for Warner-Bratzler and Slice shear force values. As pH had higher correlations with shear force values, it was not surprising that pH would be a predictor in regression equations. Jeremiah et al. (1991) used pH to predict Warner-Bratzler shear force. They reported a *P* value of 0.022 for pH and tenderness and they concluded, that pH helped to predict beef tenderness. Our study had higher R^2 values for prediction equation for Warner-Bratzler and Slice shear force when using pH with *L*, a** and *b** color space values. Our R^2 values were similar as equations reported by Wulf et al. (1997). Wulf et al. (1997) reported R^2 values of 0.18 and 0.12 when using pH and *L*, a** and *b** color space values separately. When used together, as done in our study, higher R^2 values were reported (R^2 = 0.20). Jeremiah et al. (1991) showed similar results as Wulf et al. (1997) with very low R^2 values when using pH and *L*, a** and *b** color values (0.035, 0.048, 0.092, and 0.068, respectively) separately. When pH and color space values were used in combination, R^2 values of 0.45 and 0.44 were reported. These R^2 values were higher than in our study.

Stepwise regression equations were ran using VISIBLE-NIR reflectance values, difference values, pH, and L^*, a^* and b^* color space values (Table 16). R^2 values increased for both Warner-Bratzler and Slice shear forces. Mid-range difference values again, contributed to the predictability of equations, while individual VISIBLE-NIR reflectance values contributed very little. VISIBLE-NIR reflectance values used in the equations differed from those reported by Rust et al. (2008) and Shackelford et al. (2005) who reported that reflectance values from 550 nm to 940 nm were the range of wavelengths The difference values were from the range (550 nm reflectance to 940nm reflectance) specified in the studies. L^* and b^* did not contribute to the prediction equations for 1, 7, and 14 d Warner-Bratzler shear force values, but were found to contribute to 1, 7, and 14 d Slice shear force regression equations. Warner-Bratzler shear force equations had R^2 values of 0.19 to 0.30. While Slice shear force regression equations had higher R^2 values of 0.38 to 0.44, this was higher than reported by Nath (2008) ($R^2 = 0.17$) when they used all independent variables. Nath (2008) did not use pH in that study. As our equations included pH, the variation accounted for by pH may have contributed to higher R^2 values in our equations. As mentioned before, electrical impedance values contributed little predictability to prediction equations, when used alone or in combination with VISIBLE-NIR, pH or color space values (Tables 18 and 19).

The calibration data set was sorted from toughest 14 d Warner-Bratzler shear force value to the most tender value. In this study, tough steaks were classified as > 3.9 kg, and tender were classified as < 2.7 kg. Steaks found to be between these values were

classified as intermediate. Seven steaks were classified as tough, and 297 were classified as tender. The remainders were placed in the intermediate category. The best stepwise regression equation was calculated and 14 d Warner-Bratzler shear force values were predicted. Out of the 7 toughest steaks, 0 were predicted as being tender, but 0 were predicted as being tough. All the steaks came out to be classified as intermediate. This does not compare to other studies by Price et al. (2008), Prieto, Ross, Navajas, Nute, Richardson, Hyslop, Simm, and Roehe (2009), Rust et al. (2008), and Shackelford et al. (2005). Previous studies have had high success rates in predicting beef tenderness. Rust et al. (2008) showed $P < 0.05$ for accuracy in separating tough from tender carcasses. Shackelford et al. (2005) showed a 30.1% success rate in predicting tough carcasses, but, they found a 94.5% success rate in predicting tender carcasses. Similar results were found in predicting 14 d Slice shear force values, where tough was defined as steaks with Slice shear force values > 25 kg and tender as Slice shear force values of < 15 kg. Rust et al. (2008) reported that all tender steaks were classified as tender when predicting 14 d Slice shear force values using their prediction equation.

Table 18
Stepwise regression using resistance, reactance, phase angle, and partial capacitance to predict Warner-Bratzler shear forces for 1, 7, and 14 day and Slice shear forces for 1, 7, and 14 day.

Dependent variable	Intercept	β-value	Independent variable	Partial R^2	R^2
Warner-Bratzler shear force, 1 d	17.51	0.48	Phase angle	0.02	0.02
Warner-Bratzler shear force, 7 d	15.15	0.33	Phase angle	0.01	0.01
Warner-Bratzler force, 14 d	23.47	-0.08	Resistance	0.02	0.02
		0.18	Phase angle	0.00	
Slice shear force, 1d	75.58	3.86	Phase angle	0.03	0.03
Slice shear force, 7 d	139.81	-0.58	Resistance	0.02	0.03
		1.51	Phase angle	0.01	
Slice shear force, 14 d	85.06	1.41	Phase angle	0.02	0.02

Table 19
Stepwise regression using pH, *L**, *a**, *b**, color space values resistance, reactance, phase angle, and partial capacitance to predict Warner-Bratzler shear forces for 1, 7, and 14 day and Slice shear forces for 1, 7, and 14 day.

Dependent variable	Intercept	β-value	Independent variable	Partial R^2	R^2
Warner-Bratzler shear force, 1 d	-99.54	32.84	pH	0.04	0.12
		-1.24	a*	0.03	
		0.76	b*	0.02	
		-0.56	resistance	0.01	
		1.02	reactance	0.01	
		-1.21	phase angle	0.01	
Warner-Bratzler shear force, 7 d	-150.98	41.15	pH	0.11	0.25
		-0.75	L*	0.06	
		-0.96	a*	0.09	
Warner-Bratzler shear force, 14 d	-129.28	31.71	pH	0.09	0.22
		-0.43	L*	0.04	
		-0.59	a*	0.08	
		0.00	partial capacitance	0.02	
Slice shear force, 1 d	-849.50	255.04	pH	0.04	0.20
		-6.68	L*	0.07	
		-8.10	a*	0.05	
		3.87	b*	0.01	
		1.24	reactance	0.01	
Slice shear force, 7 d	-403.28	237.15	pH	0.06	0.22
		-4.15	L*	0.07	
		-8.09	a*	0.04	
		5.44	b*	0.03	
		-4.54	resistance	0.01	
		1.95	reactance	0.01	
		-0.01	partial capacitance	0.01	
Slice shear force, 14 d	-351.14	132.05	pH	0.04	0.24
		-4.03	L*	0.10	
		-4.29	a*	0.05	
		1.87	b*	0.01	

Partial least squares regression was run using 14 d shears from Warner-Bratzler and Slice shear force values. Using VISIBLE-NIR alone, R^2 values were 0.21 for Warner-Bratzler shears, and 0.40 for Slice shears. When 14 d Warner-Bratzler shear force (Figure 2) and Slice shear force (Figure 3) values were predicted, the highest success rate was in the Slice shear force prediction equation using VISIBLE-NIR, pH, and *L**, *a** and *b** color space values. When electrical impedance was added, R^2 values decreased to 0.35 indicating that electrical impedance information did not strengthen the prediction equation. The partial least squares regression equation using VISIBLE-NIR, pH, and *L**, *a** and *b** color space values had higher R^2 values when compared to the stepwise regression equation with the same variables. There was a 20% success rate in predicting tough carcasses. For predicting intermediate carcasses, there was an 88%

success rate. The success rate was determined by taking the number of steaks predicted in the category and dividing it by the number of steaks that actually fell in that category. There was a 100% success rate in predicting the tender carcasses to be tender. However, the equation predicted 9 intermediate steaks as tender. These results are most comparable to those of Shackelford et al. (2005). For Warner-Bratzler shear forces values, there was an 85% success rate in predicting tenderness. This is higher than reported by Park et al. (1998), who showed a 79% success rate.

The VISIBLE-NIR instrument can predict tenderness and is suitable for use in the beef industry. It proved to have high success rates in predicting tender carcasses when paired with other instruments. Being able to predict tender carcasses will add value to those carcasses in the USDA Choice and Select category. However, more research needs to be done to insure more accuracy in prediction.

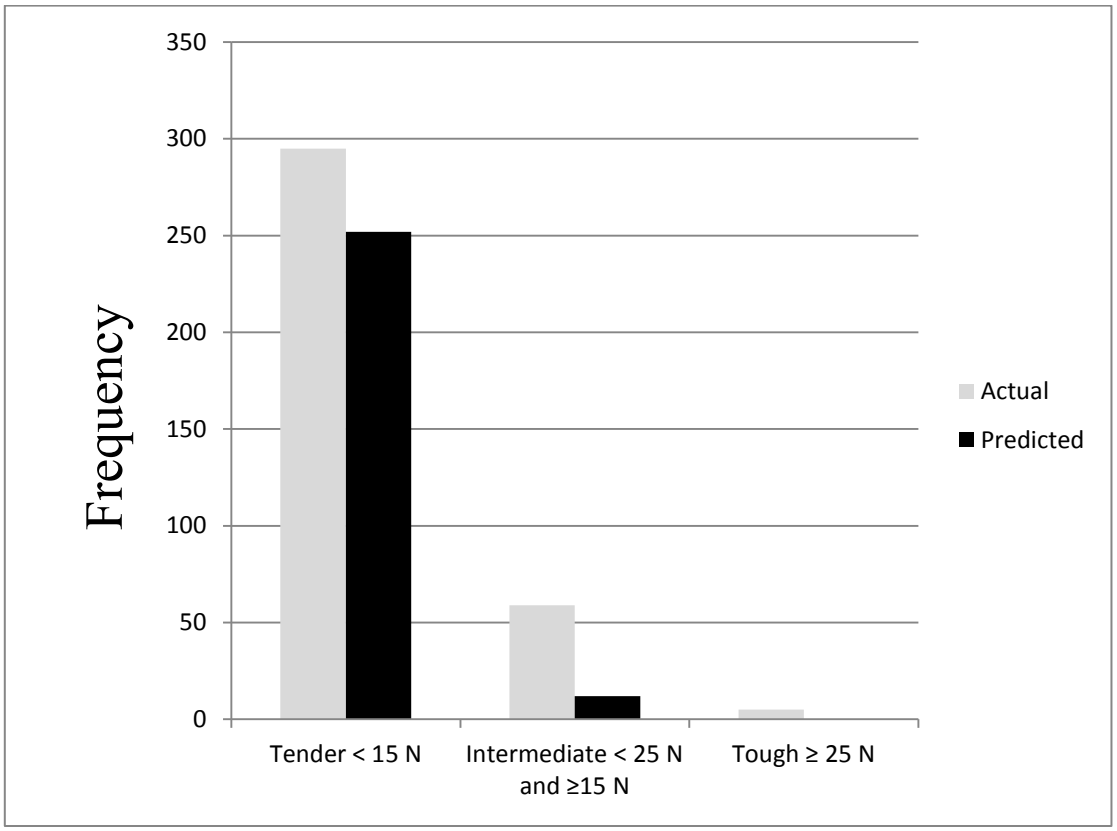

Figue 2.
Frequency numbers for actual and predicted 14 d WBSF values.

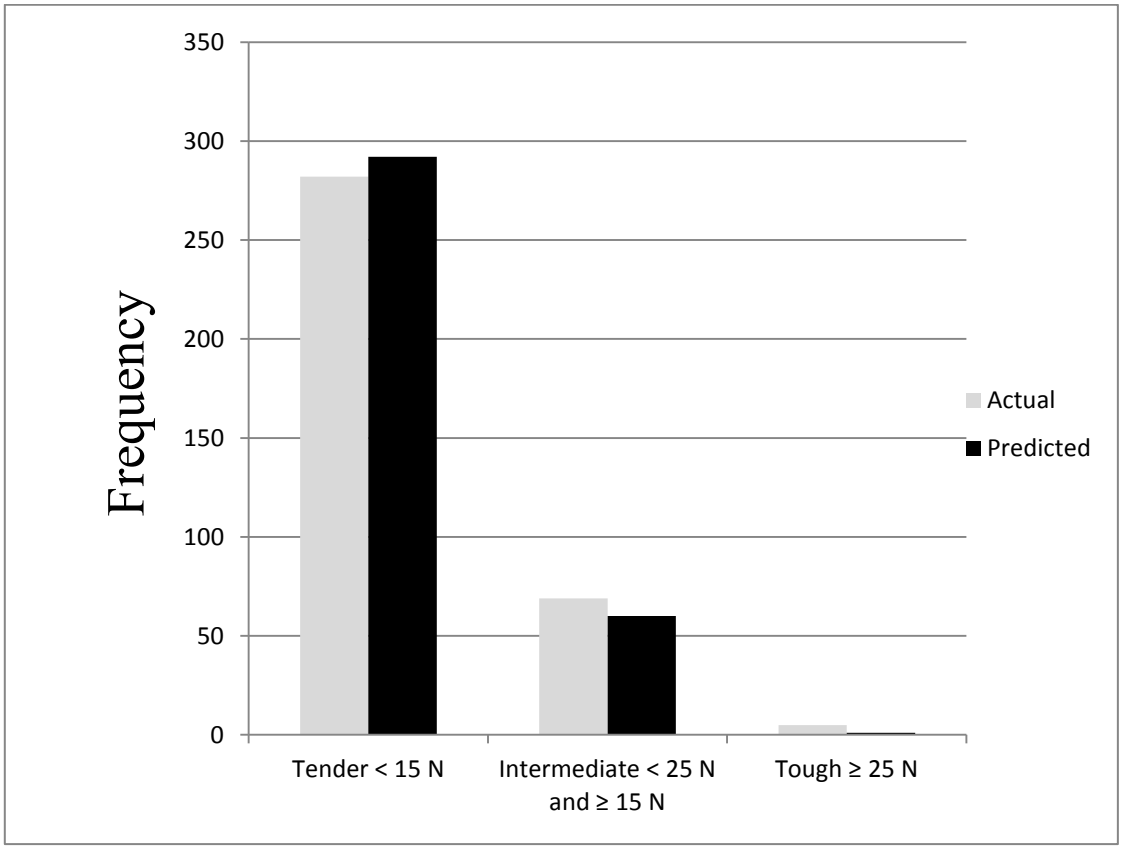

Figure 3.
Frequency numbers for actual and predicted 14 d SSF values.

REFERENCES

Andrés, S., Silva, A., Soares-Pereira, A. L., Martins, C., Bruno-Soares, A. M., & Murray, I. (2008). The use of visible and near infrared reflectance spectroscopy to predict beef M. longissimus thoracis et lumborum quality attributes. *Meat Science*, *78*(3), 217-224.

Belk, K. E. (1999). Techniques to identify palatable beef carcasses: Hunterlab Beefcam™. Available at: http://digitalcommons.unl.edu/rangebeefcowsymp/112. Accessed 18 November, 2010.

Boleman, S. J., Boleman, S. L., Miller, R. K., Taylor, J. F., Cross, H. R., Wheeler, T. L., Koohmaraie, M., Shackelford, S. D., Miller, M. F., West, R. L., Johnson, D. D., & Savell, J. W. (1997). Consumer evaluation of beef of known categories of tenderness. *Journal of Animal Science*, *75*(6), 1521-1524.

Bowling, M. B., Vote, D. J., Belk, K. E., Scanga, J. A., Tatum, J. D., & Smith, G. C. (2009). Using reflectance spectroscopy to predict beef tenderness. *Meat Science*, *82*(1), 1-5.

Brooks, J. C., Belew, J. B., Griffin, D. B., Gwartney, B. L., Hale, D. S., Henning, W. R., Johnson, D. D., Morgan, J. B., Parrish, F. C., Jr., Reagan, J. O., & Savell, J. W. (2000). National Beef Tenderness Survey-1998. *Journal of Animal Science*, *78*(7), 1852-1860.

Cross, H. R., & Whittaker, A. D. (1992). The role of instrument grading in a beef value-based marketing system. *Journal of Animal Science*, *70*, 984-989.

Garcia, L. G., Nicholson, K. L., Hoffman, T. W., Lawrence, T. E., Hale, D. S., Griffin, D. B., Savell, J. W., VanOverbeke, D. L., Morgan, J. B., Belk, K. E., Field, T. G., Scanga, J. A., Tatum, J. D., & Smith, G. C. (2008). National Beef Quality Audit-2005: Survey of targeted cattle and carcass characteristics related to quality, quantity, and value of fed steers and heifers. *Journal of Animal Science*, 3533-3543.

Geesink, G. H., Schreutelkamp, F. H., Frankhuizen, R., Vedder, H. W., Faber, N. M., Kranen, R. W., & Gerritzen, M. A. (2003). Prediction of pork quality attributes from near infrared reflectance spectra. *Meat Science*, *65*(1), 661-668.

Jeremiah, L. E., Tong, A. K. W., & Gibson, L. L. (1991). The usefulness of muscle color and pH for segregating beef carcasses into tenderness groups. *Meat Science*, *30*(2), 97-114.

Jones, B. K., & Tatum, J. D. (1994). Predictors of beef tenderness among carcasses produced under commercial conditions. *J. Anim Sci.*, *72*(6), 1492-1501.

Lepetit, J., Salé, P., Favier, R., & Dalle, R. (2002). Electrical impedance and tenderisation in bovine meat. *Meat Science*, *60*(1), 51-62.

Liao, Y.-T., Fan, Y.-X., & Cheng, F. (2010). On-line prediction of fresh pork quality using visible/near-infrared reflectance spectroscopy. *Meat Science*, *86*(4), 901-907.

NAMP. (2010). *The Meat Buyer's Guide.* Reston, VA: North American Meat Processors Association.

Nath, T. M. (2008). The use of electrical impedance to rapidly predict beef tenderness. South Dakota State University, Brookings.

Park, B., Chen, Y. R., Hruschka, W. R., Shackelford, S. D., & Koohmaraie, M. (1998). Near-infrared reflectance analysis for predicting beef longissimus tenderness. *Journal of Animal Science*, *76*(8), 2115-2120.

Price, D. M., Hilton, G. G., VanOverbeke, D. L., & Morgan, J. B. (2008). Using the near-infrared system to sort various beef middle and end muscle cuts into tenderness categories. *Journal of Animal Science*, *86*, 413-418.

Prieto, N., Ross, D. W., Navajas, E. A., Nute, G. R., Richardson, R. I., Hyslop, J. J., Simm, G., & Roehe, R. (2009). On-line application of visible and near infrared reflectance spectroscopy to predict chemical-physical and sensory characteristics of beef quality. *Meat Science*, *83*(1), 96-103.

Rødbotten, R., Nilsen, B. N., & Hildrum, K. I. (2000). Prediction of beef quality attributes from early post mortem near infrared reflectance spectra. *Food Chemistry*, *69*(4), 427-436.

Rust, S. R., Price, D. M., Subbiah, J., Kranzler, G., Hilton, G. G., Vanoverbeke, D. L., & Morgan, J. B. (2008). Predicting beef tenderness using near-infrared spectroscopy. *Journal of Animal Science*, *84*, 211-219.

Shackelford, S. D., Koohmaraie, M., Whipple, G., Wheeler, T. L., Miller, M. F., Crouse, J. D., & Reagan, J. O. (1991). Predictors of beef tenderness: Development and verification. *Journal of Food Science*, *56*(5), 1130-1135.

Shackelford, S. D., Wheeler, T. L., & Koohmaraie, M. (1999a). Evaluation of slice shear force as an objective method of assessing beef longissimus tenderness. *Journal of Animal Science*, *77*(10), 2693-2699.

Shackelford, S. D., Wheeler, T. L., & Koohmaraie, M. (1999b). Tenderness classification of beef: II. Design and analysis of a system to measure beef longissimus shear force under commercial processing conditions. *Journal of Animal Science*, *77*(6), 1474-1481.

Shackelford, S. D., Wheeler, T. L., & Koohmaraie, M. (2004). Development of optimal protocol for visible and near-infrared reflectance spectroscopic evaluation of meat quality. *Meat Science*, *68*(3), 371-381.

Shackelford, S. D., Wheeler, T. L., & Koohmaraie, M. (2005). On-line classification of US Select beef carcasses for longissimus tenderness using visible and near-infrared reflectance spectroscopy. *Meat Science*, *69*(3), 409-415.

Shackelford, S. D., Wheeler, T. L., Meade, M. K., Reagan, J. O., Byrnes, B. L., & Koohmaraie, M. (2001). Consumer impressions of Tender Select beef. *Journal of Animal Science*, *79*(10), 2605-2614.

USDA. (1997). United States Standards for Grades of Carcass Beef. Available at: http://www.ams.usda.gov/AMSv1.0/getfile?dDocName=STELDEV3002979. Accessed 10/20/10.

Vote, D. J., Belk, K. E., Tatum, J. D., Scanga, J. A., & Smith, G. C. (2003). Online prediction of beef tenderness using a computer vision system equipped with a BeefCam module. *Journal of Animal Science*, *81*(2), 457-465.

Wheeler, T. L., Vote, D. J., Leheska, J. M., Shackelford, S. D., Belk, K. E., Wulf, D. M., Gwartney, B. L., & Koohmaraie, M. (2002). The efficacy of three objective systems for identifying beef cuts that can be guaranteed tender. *Journal of Animal Science*, *80*(12), 3315-3327.

Wulf, D. M., O'Connor, S. F., Tatum, J. D., & Smith, G. C. (1997). Using objective measures of muscle color to predict beef longissimus tenderness. *Journal of Animal Science*, *75*(3), 684-692.

Wulf, D. M., & Page, J. K. (2000). Using measurements of muscle color, pH, and electrical impedance to augment the current USDA beef quality grading standards and improve the accuracy and precision of sorting carcasses into palatability groups. *Journal of Animal Science*, *78*(10), 2595-2607.

Wulf, D. M., & Wise, J. W. (1999). Measuring muscle color on beef carcasses using the L*a*b* color space. *Journal of Animal Science*, *77*(9), 2418-2427.

Wyle, A. M., Vote, D. J., Roeber, D. L., Cannell, R. C., Belk, K. E., Scanga, J. A., Goldberg, M., Tatum, J. D., & Smith, G. C. (2003). Effectiveness of the

SmartMV prototype BeefCam System to sort beef carcasses into expected palatability groups. *J. Anim Sci.*, *81*(2), 441-448.

Yancey, J. W. S., Apple, J. K., Meullenet, J. F., & Sawyer, J. T. (2010). Consumer responses for tenderness and overall impression can be predicted by visible and near-infrared spectroscopy, Meullenet-Owens razor shear, and Warner-Bratzler shear force. *Meat Science*, *85*(3), 487-492.

VITA

William Al Wiederhold received his Bachelor of Science degree in Animal Science at Texas A&M University in College Station in 2008. He entered the Meat Science program in August 2008 where he received his Master of Science degree in 2011. His research interests include predicting tenderness, product development, and food safety. He plans to pursue a career the industry and has currently accepted a job offer with Eddy Packing Co. in Yoakum, Texas.

Mr. Wiederhold may be reached at 404 Airport Drive, Yoakum, TX 77995. His email is WAWZ71@aol.com